



Article

Pyrolytic Depolymerization Mechanisms for Post-Consumer Plastic Wastes [†]

Kirtika Kohli ^{1,2}, Sriraam R. Chandrasekaran ², Ravindra Prajapati ², Bidhya Kunwar ², Sultan Al-Salem ³ , Bryan R. Moser ⁴ and Brajendra K. Sharma ^{2,5,*} 

¹ Aromatic Separation Area, Separation Process Division, CSIR-Indian Institute of Petroleum, Dehradun 248005, Uttarakhand, India

² Prairie Research Institute—Illinois Sustainable Technology Center, University of Illinois Urbana Champaign, Champaign, IL 61820, USA

³ Environment & Life Science Research Center, Kuwait Institute for Scientific Research (KISR), Safat 13109, Kuwait

⁴ Bio-Oils Research Unit, National Center for Agricultural Utilization Research, Agricultural Research Service, United States Department of Agriculture, 1815 N. University St., Peoria, IL 61604, USA

⁵ Sustainable Biofuels and Co-Products Research Unit, Eastern Regional Research Center, Agricultural Research Service, United States Department of Agriculture, Wyndmoor, PA 19038, USA

* Correspondence: brajendra.sharma@usda.gov

[†] Mention of trade names or commercial products in this article is solely for the purpose of providing specific information and does not imply recommendation or endorsement by the U.S. Department of Agriculture. USDA is an equal opportunity provider and employer.

Abstract: Fast pyrolysis of five post-consumer plastic waste materials was studied using pyrolysis coupled with gas chromatography/mass spectrometry (Py-GC/MS) technique. Prescription medicine bottles, landfill liners, and one type of industrial plastic waste represented polyolefin-based polymers, whereas packaging material represented polystyrene, and other industrial plastic waste represented polyurethane. The noncatalytic and catalytic degradation mechanisms of all five post-consumer plastic wastes were elucidated. The noncatalytic pyrolysis experiments were conducted at a temperature of 600 °C for a residence time of 5 min. For catalytic pyrolysis, a spent FCC catalyst was utilized for polystyrene, a sulfated zirconia-based catalyst was utilized for polyurethane, and a Y-zeolite catalyst was used for polyolefinic plastic waste. The results suggested that the thermal reaction has higher monomeric and oligomeric selectivity than the catalytic reaction. Results from the catalytic runs showed that the addition of catalysts greatly influences product compositions and has a significant effect on the selectivity of a specific compound. One of the plastic wastes, landfill liner, was selected for a batch scale pyrolysis at 420–440 °C using Y-zeolite as a catalyst to demonstrate the product properties and potential use of the liquid product formed. The complete product distribution of plastic crude oil was performed followed by distillation to produce aviation range fuel. The fuel properties of aviation range fuel were examined, and results suggested that the fuel fraction can be easily blended with commercially available fuels for direct applications.

Keywords: plastic wastes; thermal decomposition; pyrolysis; catalysts; degradation mechanism; Py-GC/MS



Citation: Kohli, K.; Chandrasekaran, S.R.; Prajapati, R.; Kunwar, B.; Al-Salem, S.; Moser, B.R.; Sharma, B.K. Pyrolytic Depolymerization Mechanisms for Post-Consumer Plastic Wastes. *Energies* **2022**, *15*, 8821. <https://doi.org/10.3390/en15238821>

Academic Editor: Javier Fermoso

Received: 28 September 2022

Accepted: 15 November 2022

Published: 23 November 2022

Publisher's Note: MDPI stays neutral with regard to jurisdictional claims in published maps and institutional affiliations.



Copyright: © 2022 by the authors. Licensee MDPI, Basel, Switzerland. This article is an open access article distributed under the terms and conditions of the Creative Commons Attribution (CC BY) license (<https://creativecommons.org/licenses/by/4.0/>).

1. Introduction

By 2015, a total of 8.3 billion metric tons of plastics had been manufactured worldwide and 6.3 billion tons of plastic waste had been generated [1], almost half of which was dumped in landfills and the environment. Projected data indicate that, by 2025, 26 billion tons of plastic waste will be produced [1]. The buildup of plastic waste in the environment is a growing global concern. Plastics constitute a low-cost, hydrophobic, bioinert, easily formable, and high-modulus material that is widely used in our daily lives and different consumer products. Figure 1 presents the worldwide plastic waste generation

by industrial sector in 2015. Packaging materials (PMs) are the main contributor to plastic waste, representing ~42% of the global annual resin production [2]. An increase in population and the future use of plastics will cause the amount of post-consumer plastic waste to escalate tremendously. Another report by the US Environmental Protection Agency (EPA) [3] showed that, of the plastic wastes generated, 5.6% is from the PM sector (polyethylene terephthalate bottles and jars; high-density polyethylene (HDPE) bottles and jars; bags, sacks, and wraps; other containers), 4.4% is durable goods (plastics in appliances; wide range of resins), and 2.7% is nondurable goods (plates and cups; trash bags). Hoornweg et al. [4] reported that, by 2025, the global urban population is estimated to generate >6 million tons per day of solid waste (SW). This is becoming a major concern for the solid waste management industry (SWMI) on account of the growing cost of land-filling [5]. In order to minimize plastic waste and ensure environmental protection, plastic recycling methods are continuously developing.

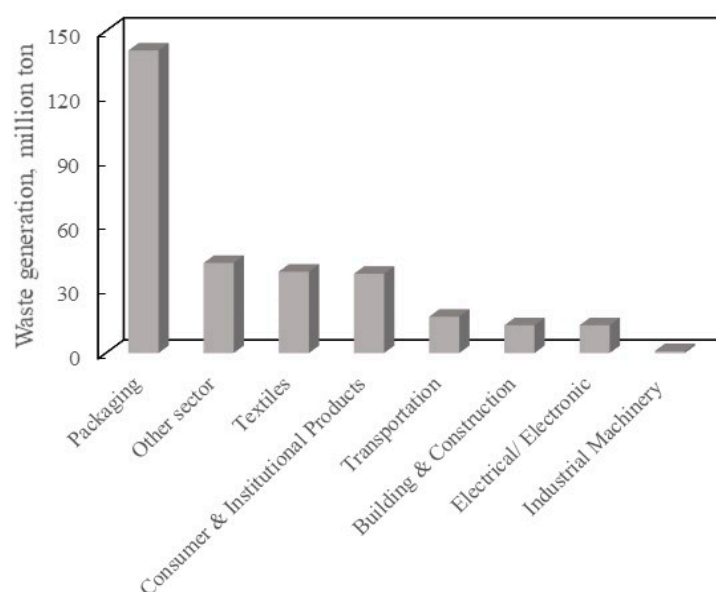


Figure 1. Global plastic waste generation by industrial sector in 2015 [2].

Pyrolysis is an attractive route to recycle plastic waste by treating plastic materials to produce feedstock for the petroleum and petrochemical industries [6–10]. In the petroleum refinery catalytic cracker unit, the feedstock can be used to produce gasoline. This feedstock can also be used in a steam cracker to produce alkenes, which are used to make new plastics. Several reports are available in the literature on the pyrolysis of individual types of plastics [7,8] and mixtures of plastics [9,10] to generate either a fuel product or a petrochemical feedstock. Pyrolysis can be performed with (catalytic) and without catalyst (noncatalytic). Catalytic pyrolysis is found to be more advantageous as catalysts promote the degradation reactions at lower temperatures, which leads to lower energy consumption [11–14]. In addition, the shape-selective nature of the catalysts leads to the formation of selective products, such as value-added hydrocarbons, fuels, and chemicals with higher market values. Zhang et al. [15] disclosed that the degradation temperature of plastic wastes can be decreased in the presence of a ZSM-5 catalyst, as catalytic cracking decreases the overall activation energy for the process. Similarly, other researchers [16,17] reported the production of high-quality oil with a large amount of aromatic hydrocarbons using catalytic pyrolysis of plastics. Jia et al. [18] investigated the PE liquid-phase hydrogenolysis to liquid fuels using a Ru/C catalyst in the presence of a solvent (hexane). The experimental results demonstrated that 90 wt.% HDPE was converted to C₈⁺ liquid hydrocarbon product at 220 °C, 30 bar H₂ pressure, and 1 h residence time. The product distribution can be tuned by adjusting the reaction conditions such as reaction temperature, time, catalyst loading, and hydrogen pressure. Tomasek et al. [19] investigated the production of jet fuel

from a mixture of cracked material (having a mixture of polyethylene (PE), polypropylene (PP), and straight-run kerosene) in the presence of NiMo/Al₂O₃/P catalyst. The authors concluded that the existing hydrogenation plants are suitable to produce jet fuels from cracked waste PP fractions and straight-run kerosene through a single step, with 16–64% energy saving. However, with cracked PE fraction as a feedstock, one more step, i.e., hydroisomerization is needed before the application. In general, catalytic pyrolysis of plastic waste produces a complex and nonhomogeneous mixture of hydrocarbons (C₆ to >C₂₅ carbon numbers) and these must undergo further downstream upgrading steps to produce finished fuel or chemicals. Most recently, Peng et al. [20] reviewed the catalytic pyrolysis of plastic waste to produce high-value products and their full utilization to build the required technological and economic push for a circular economy. Dai et al. [21] reviewed various recovery pathways of plastic waste pyrolysis for various products (such as fuels, light olefins, naphtha, and hydrogen). The effect of waste plastic pyrolysis oil, n-butanol, nanoparticles (hybrid Al₂O₃ and TiO₂), and diesel fuel blends on combustion, toxic particulates, and gaseous emissions from CRDI diesel engines in a steady-state mode was investigated [22]. The results showed that significant benefit could be attained using the fuel mixtures in the presence of nanoparticles at relatively higher concentrations.

To develop a better and more effective process for plastic waste recycling, it is most important to identify (a) what kinds of polymers are present and (b) how the impurities or additives present in plastic wastes affect the recycling processes, because these processes can be improved by better separation and processing techniques. Different techniques, such as Fourier-transform infrared (FT-IR), Raman, thermogravimetric analysis (TGA), and pyrolysis coupled with gas chromatography/mass spectrometry (Py-GC/MS), are frequently used to identify the polymer types and impurities present in plastic wastes [23–31]. Among these, Py-GC/MS is an important analytical tool that can provide fundamental information to develop recycling methods for plastic wastes and characterize plastics. Py-GC/MS analysis assesses all aspects of plastic wastes in contrast to the FT-IR and Raman techniques, which mainly analyze the surface of the plastic materials and may be unable to assess the interference caused by additives or impurities present in plastic wastes. TGA provides information regarding mass changes in the samples with heat treatment under controlled conditions. Our earlier work discussed the noncatalytic and catalytic pyrolysis of five types of plastic wastes using TGA [14]. However, the study does not provide any chemical information about the materials.

Thus, in the present study, five different types of plastic wastes (made of polyolefin, polystyrene, and polyurethane polymers), i.e., packaging materials, landfill liners, two industrial plastic wastes, and medicine bottles from different sources, were selected to study noncatalytic and catalytic degradation products using the Py-GC/MS technique. The contaminants present in the plastic wastes can possibly redirect the noncatalytic and catalytic pyrolysis decomposition, and the effect of these contaminants can be quickly and easily determined using Py-GC/MS. In addition to the investigation of these pyrolytic degradation products, this study provides insight into the reaction mechanism under catalytic conditions and different pyrolysis temperatures. Translation of learnings from these experiments to batch-scale pyrolysis of one of the plastic wastes is also demonstrated by producing fuel in the range of gasoline and aviation fuel through the distillation of liquid plastic crude oil. A detailed fuel property analysis and comparison with commercial aviation fuel showed that the aviation range fuel fraction could be blended with aviation fuel and meets some of the ASTM specifications. The novelty of this work is the elucidation of the reaction mechanism of noncatalytic and catalytic depolymerization of plastic wastes.

2. Materials and Methods

2.1. Materials

Post-consumer plastic wastes such as landfill liners (LL), prescription medicine bottles (MB), packaging materials (PM), and two industrial plastic wastes (IPW1 and IPW2) were taken from a materials recovery facility. For the present work, these materials were ground

to a particle size of <2 mm using an AEC Nelmor shredder (Blade machinery Co., Inc., Elk Grove Village, IL, USA). Y-zeolites, sulfated zirconia, and fluid catalytic cracking (FCC) spent catalysts were procured from Sigma-Aldrich (St. Louis, MO, USA) and utilized as such for the research work. The designations and catalysts used in the catalytic pyrolysis are reported in Table 1. According to the results from a previous study using TGA [14], Y-zeolites were used for the catalytic pyrolysis of polyolefinic plastic wastes LL, IPW1, and MB materials, while FCC spent catalyst was used for the catalytic pyrolysis of PM, and sulfated zirconia was used for IPW2. The elemental properties of plastic wastes were described elsewhere [14].

Table 1. Description of plastic waste materials and catalyst used for the Py-GC/MS study.

Plastic Waste Material	Catalyst Used	Designation Used
Polyolefinic plastic waste		
Landfill liners	Y-zeolite	LL
Industrial plastic waste 1	Y-zeolite	IPW1
Medicine bottles	Y-zeolite	MB
Polystyrene plastic waste		
Packaging material	FCC spent catalyst	PM
Polyurethane plastic waste		
Industrial plastic waste 2	Sulfated zirconia	IPW2

2.2. Pyrolysis-GC/MS Experiments

The pyrolysis experiment was performed in a CDS 5000 pyroprobe device directly connected to an ion trap Varian 3800 GC with a Varian MS (GC/MS-3800). For each experiment, 100 to 200 µg of grounded plastic waste samples were placed into a quartz tube. Glass wool was placed on both ends of the tube. The pyrolyzer was operated in trap mode under a helium atmosphere. The transfer lines and valve oven were maintained at 325 °C to prevent condensation. The volatile pyrolysis products were separated on a capillary column RTX5-MS (30 m long, 0.25 mm ID, and 0.25 µm film thickness). The carrier gas used was helium (1 mL/min). The initial oven temperature was 40 °C and was subsequently increased to 300 °C at a rate of 5 °C/min. The MS was operated in EI mode (70 eV) over the range of 40–500 Da. The inlet auxiliary lines were both maintained at 300 °C, and the ion source was kept at 230 °C. The product compositions in terms of peak area percentage relative content of the components were determined using the area normalization method. All peaks were identified using the NIST Research Library.

The noncatalytic pyrolysis experiments were conducted at a reaction temperature of 600 °C with 5 min of residence time. For the catalytic runs, the catalyst was placed on either side of the sample, followed by glass wool in the quartz tube. The catalytic pyrolysis was studied at 600 °C and 500 °C reaction temperatures. The catalyst-to-sample ratio of 1:10 was chosen on the basis of our optimization study conducted on TGA [14].

2.3. Batch-Scale Pyrolysis of Landfill Liner

In order to mimic fast pyrolysis in a batch process, pyrolysis of landfill liners (real plastic waste) was conducted in a benchtop plastic to oil pyrolysis unit at optimized conditions and catalyst as described in detail earlier [32]. Briefly, 500 g of plastic waste was pyrolyzed at a temperature in the presence of Y-zeolite. The pyrolysis reactor had two heating zones: upper (set at 420 °C) and lower (440 °C). Once the reactor reached the set temperatures, a reaction time of 120 min was counted from that point on. Vapors produced during the pyrolysis were condensed over water as plastic crude oil (PCO). The upper oil layer was separated and weighed (81% yield). After cooling the reactor (<50 °C), the reactor lid was opened to remove the residue solid material. The weight of residual material recovered was 5%. The mass balance yields were calculated as the ratio of the corresponding product phase obtained to the initial feedstock weight. The gas phase yield (14%) was calculated on the basis of the resulting mass difference. The experimental details are described elsewhere [32,33].

The products obtained after the pyrolysis were (i) gaseous product, (ii) liquid product (referred as PCO), and (iii) solid residue, which remained at the bottom of the reactor system. For more clarity, the plastic crude oil is designated as PCO-LL, indicating plastic crude oil derived from landfill liner plastic waste. PCO-LL was distilled using an automated 36–100 spinning band distillation system (BR instrument, Easton, MD) into fractions; the ~25% gasoline range (<150 °C), ~45% aviation range fuel (150–275 °C), and ~24% gas oil plus range, i.e., >275 °C containing gas oil and vacuum gas oil, as described elsewhere [33].

2.3.1. Product Analysis

The elemental analysis of the LL and PCO-LL fractions was performed at the University of Illinois Microanalysis Laboratory (Urbana, IL, USA). An Exeter Analytical (Chelmsford, MA, USA) CE-440 Elemental Analyzer was used for the total CHN (carbon/hydrogen/nitrogen) analysis. Oxygen was determined by mass balance closure. The chemical functional group analysis was carried out using Fourier-transform infrared (FT-IR) and nuclear magnetic resonance (NMR) spectroscopies. FT-IR spectra were recorded on a Thermo-Nicolet Nexus 470 FT-IR spectrometer (Madison, WI) with a Smart ARK accessory containing a 45 ZeSe trough in a scanning range of 650–4000 cm^{-1} for 64 scans at a spectral resolution of 4 cm^{-1} . ^1H -NMR spectra were collected using a Bruker Avance-500 spectrometer (Billerica, MA) running Topspin 1.4 p18 software operating at 500 MHz using a 5 mm BBO probe. Samples were dissolved in deuterated chloroform (CDCl_3), and all spectra were acquired at 27 °C.

Hydrocarbon composition was identified utilizing an Agilent (Palo Alto, CA, USA) model 7890 GC equipped with a model 7683 auto-injector and a model 5975 MSD in an electron impact mode. An Agilent DB-35MS column (30 m \times 0.320 mm; 0.25 μm film thickness) was used with a helium flow rate of 0.509 mL/min. The temperature program began with a hold at 30 °C for 10 min followed by an increase at 1 °C/min to 195 °C, followed by 35 °C/min to 330 °C, which was held for 1 min. The injector and column transfer line heater were both set to 340 °C. The detector inlet and MS quadrupole temperature were 220 and 150 °C, respectively. The injection volume was 1 μL with a split ratio of 50:1. Samples (5 mg) were dissolved in heptane (1 mL). Identification of chromatographic peaks was performed using their MS fragmentation profile and matched with Agilent and NIST spectral library.

2.3.2. Fuel Properties Analysis

Properties were measured ($n = 3$) following AOCS, ASTM, and EN standard test methods using instrumentation described previously [34–36]: cloud point (CP, °C), ASTM D5773; pour point (PP, °C), ASTM D5949; cold filter plugging point (CFPP, °C), ASTM D6371; induction period (IP, h), EN 15751; kinematic viscosity (KV, cSt), ASTM D445; specific gravity (SG), ASTM D4052; density (kg/m^3), ASTM D4052; acid value (AV, mg KOH/g), AOCS Cd 3d-63; and gross heat of combustion (higher heating value, HHV, MJ/kg), ASTM D4809. Surface tension (mN/m) was measured as described by Doll et al. [37].

3. Results

The noncatalytic (thermal) fast pyrolysis of polyolefinic plastic waste materials (LL, IPW1, and MB) was performed at 600 °C. The comparison of noncatalytic and catalytic pyrolysis of the polyolefinic plastic wastes is discussed below. Similarly, the fast pyrolysis of PM and IPW2 plastic wastes is also explained separately.

3.1. Landfill Liners (LL) Pyrolysis

The noncatalytic pyrolysis of LL at 600 °C showed the formation of 34% bibenzyl, 17% tritetracontane (long-chain hydrocarbon), and 13% diphenylmethane as the main compounds (shown in Table 2). On the basis of the identified decomposition products, the plastic was identified as PE. The main feature of the pyrolysis of PE is the formation of saturated aliphatic, unsaturated, and aromatic hydrocarbons. The catalytic pyrolysis with

Y-zeolite as a catalyst at 600 °C showed the formation of alkene and aliphatic compounds, such as 12% 4-undecene-5-methyl and 23% nonadecane, respectively. In addition, aromatic compounds such as 20% 3-butynylbenzene, 8.5% diphenylacetylene, 7% biphenylene, 4.2% phenanthrene-1-methyl, and 2.5% anthracene were detected. At a pyrolysis temperature of 500 °C, mainly aromatic compounds were formed. For example, naphthalene-1-methyl (33%), biphenylene (20.5%), and acenaphthalene (11.3%) were formed at 500 °C. The zeolitic pyrolysis products suggest that the catalyst behaved differently at the different reaction temperatures used. At a lower temperature, it led mainly to the formation of aromatic hydrocarbons; however, at 600 °C, saturated compounds were formed. As per a literature report [38], US-Y, Y, and β zeolites mainly produce alkanes, while with mordenite and ZSM-5, the major products are alkenes. This occurs because of the rapid bimolecular hydrogen transfer reactions that lead to the production of saturated hydrocarbons [38].

Table 2. Analysis of landfill liner by Py-GC/MS with and without Y-zeolite catalyst.

Compound Name	Formula (Molecular Weight, g/mol)	Area, %		
		Without Catalyst	With Y-Zeolite Catalyst	
		at 600 °C	at 600 °C	at 500 °C
Cyclopropane-1,1-dimethyl-	C ₅ H ₁₀ (70)	-	-	1.23
4-undecene-5-methyl	C ₁₂ H ₂₄ (168)	3.14	11.94	-
Azulene	C ₁₀ H ₈ (128)	-	-	4.99
Tritetracontane	C ₄₃ H ₈₈ (604)	17.02	-	-
Benzene-1,3-bis(1,1-dimethylethyl)-	C ₁₄ H ₂₂ (190)	9.36	4.09	1.12
2-tridecenal	C ₁₃ H ₂₄ O (196)	-	1.39	-
Decane-2,3,5,8-tetramethyl-	C ₁₄ H ₃₀ (198)	-	-	0.36
Naphthalene-1-methyl-	C ₁₁ H ₁₀ (142)	-	-	33.06
Cyclopentane-1-pentyl, 2-propyl-	C ₁₃ H ₂₆ (182)	6.03	-	-
Pent-1-yn-3-ene, 4-methyl-3-phenyl-	C ₁₂ H ₁₂ (156)	-	2.24	1.30
Biphenyl	C ₁₂ H ₁₀ (154)	1.80	2.87	7.28
Acenaphthalene	C ₁₂ H ₁₀ (154)	-	-	11.27
Diphenylmethane	C ₁₃ H ₁₂ (168)	13.07	3.43	-
Biphenylene	C ₁₂ H ₈ (152)	-	7.12	20.48
Cyclohexane-1,2,4,5-tetraethyl	C ₁₄ H ₂₈ (196)	2.16	1.38	-
4-nonene-5-butyl-	C ₁₃ H ₂₆ (182)	-	1.45	-
Bibenzyl	C ₁₄ H ₁₄ (182)	34.34	-	-
Stilbene	C ₁₄ H ₁₂ (180)	-	2.27	2.46
Fluorene	C ₁₃ H ₁₀ (166)	-	-	0.77
Heptane-1,1-dicyclohexyl-	C ₁₉ H ₃₆ (264)	-	-	0.20
3,5-dodecadiene-2-methyl-	C ₁₃ H ₂₄ (180)	-	1.56	-
Diphenylacetylene	C ₁₄ H ₁₀ (178)	-	8.54	0.28
2-methyltetracosane	C ₂₅ H ₅₂ (352)	-	-	9.36
Nonadecane	C ₁₉ H ₄₀ (269)	-	22.92	-
3-butynylbenzene	C ₁₀ H ₁₀ (130)	8.32	20.37	3.21
4-isopropylidicyclohexylmethane	C ₁₆ H ₃₀ (222)	-	1.77	-
Phenanthrene-1-methyl-	C ₁₅ H ₁₂ (192)	-	4.20	1.55
1-nonadecene	C ₁₉ H ₃₈ (266)	4.78	-	-
Anthracene		-	2.47	1.07

Proposed mechanism: In general, in the pyrolysis of polyolefins (e.g., PE) that contain mainly C–H and C–C bonds, the chain initiation step occurs by breaking the polymeric chain, with consequent stabilization of the free radicals formed. Secondary free radicals are formed by the hydrogen abstraction from the neighboring molecules, which later undergo β -scission to generate an unsaturated end-group, as shown in Figure 2a [39–41].

In the present study, the thermal degradation of LL involved the breaking of C–C bonds in the polymeric chain, and this cracking could occur through random scission at any position of the chain or in its extremities [39]. This led to the formation of mainly aromatic compounds during noncatalytic pyrolysis (reaction mechanism shown in Figure 2). It was observed that the catalytic pyrolysis at 600 °C mainly formed alkanes, alkenes, and their

branched derivatives. This could occur via either the carbenium ion mechanism or hydride ion abstraction [42]. The different acid sites present in the catalyst, such as Brønsted and Lewis, are mainly responsible for these mechanisms. De Stefanis et al. [41] reported that polyethylene catalytic degradation involves the carbenium ion mechanism or hydride ion abstraction. The carbenium ion mechanism occurs via proton addition (Brønsted acid sites) to C–C bonds of polyethylene molecules, while hydride ion abstraction proceeds via Lewis acid sites. This ultimately proceeds toward the formation of aliphatic hydrocarbon molecules.

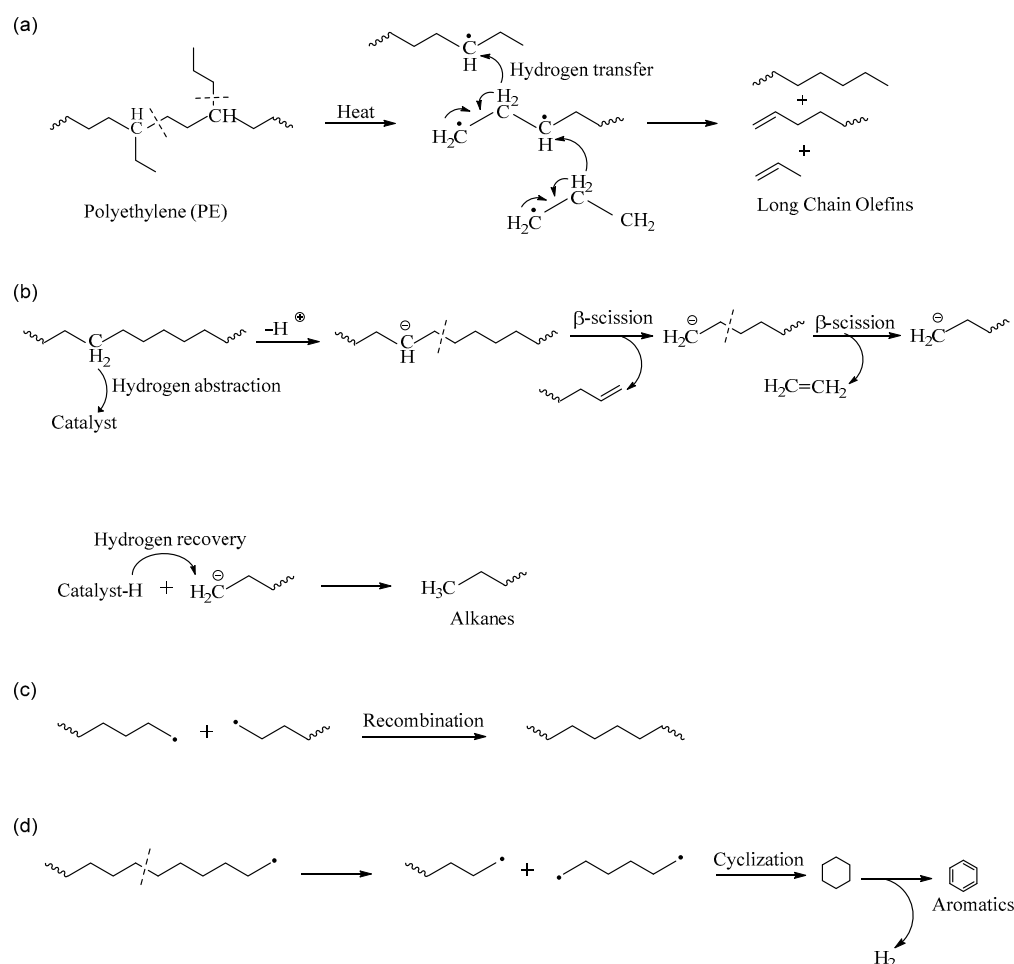


Figure 2. Reaction mechanism involved for the noncatalytic and catalytic pyrolysis of polyethylene present in landfill liners. (a) free radical chain scission and hydrogen transfer to form olefins; (b) hydrogen abstraction and β -scission followed by chain termination through proton recovery; (c) free radical chain termination through recombination to form long chain alkanes; (d) chain scission followed by cyclization and dehydrogenation to form aromatics.

The formation of aromatic compounds in catalytic pyrolysis at a lower temperature (500 °C) might have been due to the random scission in the polymeric backbone instead of the C–C backbone initiation scission [6,7]. As the chain initiation reactions might have varied at the lower reaction temperature, this led to the condensation of the polymeric structure and the formation of aromatic hydrocarbons. Another reason for the formation of aromatic compounds might have been the presence of fillers and additives that are mainly added to plastic materials to prevent long-term degradation of the polymers. The degradation of these additives might have been difficult at a lower reaction temperature; therefore, aromatic compounds were formed.

3.2. Industrial Plastic Waste 1 (IPW1) Pyrolysis

Table 3 shows the Py-GC/MS product distribution acquired from the noncatalytic and catalytic pyrolysis of IPW1. The major compounds formed during the noncatalytic pyrolysis of IPW1 at 600 °C were alkenes such as 13% 1-nonadecene, 10% hexacosene, 4% 7-tetradecene, 4% 2-hexene-5-methyl, and 3% 1-decene. In addition, alkynes such as 9-octadecyne (6%) and 1-hexadecyne (1.4%), and cycloalkanes such as cyclododecane (7.7%) and cyclopentane-1,2-dimethyl (3%) were found. The alkanes 12% decane-2,3,5,8-tetramethyl and 2.6% nonadecane were also detected. The noncatalytic Py-GC/MS product from IPW1 highlighted the resemblance of this plastic waste material to PE. Surprisingly, when the pyrolysis was performed with Y-zeolite at 600 °C, mostly aromatic compounds were formed. The detected aromatic compounds were benzocycloheptatriene (18%), biphenylene (14%), biphenyl (13%), naphthalene-2,3-dimethyl (8%), 3-butynylbenzene (6%), and phenanthrene-1-methyl (5.5%). This product distribution resembled LL plastic waste, and both waste materials LL and IPW1 resembled PE plastics. The major difference between these two plastic waste materials was in the noncatalytic pyrolysis of LL and IPW1 at the same temperature. In the case of the noncatalytic pyrolysis of LL, mainly aromatic compounds were formed, whereas, during thermal pyrolysis of IPW1, various alkenes, alkynes, cycloalkanes, and alkanes were formed. These results indicate that, although both materials resembled PE, presence and concentration of different impurities, such as fillers/additives may have been responsible for the differences in the product composition during thermal pyrolysis at the same reaction conditions. Similar products were formed during the catalytic pyrolysis at 600 °C, suggesting that Y-zeolite is effective as a catalyst for the pyrolysis of polyolefins to aromatic compounds, even if impurities are present in the plastic waste materials. The reaction mechanism involved for IPW1 resembled the mechanism described in the pyrolysis of LL.

Table 3. Analysis of industrial plastic waste 1 by Py-GC/MS with and without Y-zeolite catalyst.

Compound Name	Formula (Molecular Weight, g/mol)	Area, %		
		Without Catalyst	With Y-Zeolite Catalyst	
		at 600 °C	at 600 °C	at 500 °C
2-hexene-5-methyl-	C ₇ H ₁₄ (98)	4.17	-	-
Cyclopentane-1,2-dimethyl	C ₇ H ₁₅ (98)	2.94	-	-
Tritetracontane	C ₄₃ H ₈₈ (604)	6.64	0.97	2.59
1-decene	C ₁₀ H ₂₀ (140)	3.25	-	-
7-tetradecene	C ₁₄ H ₂₈ (196)	4.66	3.96	4.30
1-nonene-4,6,8-trimethyl-	C ₁₂ H ₂₄ (168)	0.97	-	-
1,6-heptadiene-3,3-dimethyl	C ₉ H ₁₆ (124)	-	0.57	-
4-decyne	C ₁₀ H ₁₈ (138)	0.50	-	-
Decane-2,3,5,8-tetramethyl-	C ₁₄ H ₃₀ (198)	11.78	6.86	2.34
6-dodecyne	C ₁₂ H ₂₂ (166)	3.83	-	1.92
9-octadecene	C ₁₈ H ₃₆ (252)	9.09	-	1.62
Cyclododecane	C ₁₂ H ₂₄ (168)	7.73	-	0.61
Azulene	C ₁₀ H ₈ (128)	-	-	5.73
Cyclotetradecane	C ₁₄ H ₂₈ (196)	3.58	-	-
7-hexadecyne	C ₁₆ H ₃₀ (222)	1.43	-	-
1-nonadecene	C ₁₉ H ₃₈ (266)	13.26	-	-
Cyclopentane-1-pentyl-2-propyl-	C ₁₃ H ₂₆ (182)	-	-	7.30
Benzocycloheptatriene	C ₁₁ H ₁₀ (142)	-	17.76	14.32
Cyclooctene-3-methyl-	C ₉ H ₁₆ (124)	1.37	-	-
Hexane-1-(isopropylidenecyclopropyl)	C ₁₂ H ₂₂ (166)	-	-	1.24
Biphenyl	C ₁₂ H ₁₀ (154)	-	13.07	4.70
4,4-dipropylheptane	C ₁₃ H ₂₈ (184)	-	-	2.06
Naphthalene-2,3-dimethyl-	C ₁₂ H ₁₂ (156)	-	7.93	14.17
Acenaphthalene	C ₁₂ H ₁₀ (154)	-	2.38	1.20

Table 3. Cont.

Compound Name	Formula (Molecular Weight, g/mol)	Area, %		
		Without Catalyst	With Y-Zeolite Catalyst	
		at 600 °C	at 600 °C	at 500 °C
Diphenylmethane	C ₁₃ H ₁₂ (168)	-	9.94	-
Biphenylene	C ₁₂ H ₈ (152)	-	13.84	6.21
2-octene-2,3,7-trimethyl-	C ₁₁ H ₂₂ (154)	-	-	1.66
Cyclopentane-1,1,3,4-tetramethyl	C ₉ H ₁₈ (126)	-	1.52	-
cis stilbene	C ₁₄ H ₁₂ (180)	-	-	4.03
Bibenzyl	C ₁₄ H ₁₄ (182)	-	1.56	-
2-undecene-4,5-dimethyl-	C ₁₃ H ₂₆ (182)	-	-	0.76
9-octadecyne	C ₁₈ H ₃₄ (250)	5.59	3.28	-
2-methyltetracosane	C ₂₅ H ₅₂ (352)	-	-	2.09
Anthracene-1,2-dihydro	C ₁₄ H ₁₂ (180)	-	4.88	1.67
3-butynylbenzene	C ₁₀ H ₁₀ (130)	-	5.96	4.63
Nonadecane	C ₁₉ H ₄₀ (268)	2.60	-	2.46
Phenanthrene-1-methyl-	C ₁₅ H ₁₂ (152)	-	5.52	10.23
Cyclohexane-tricosyl-	C ₂₉ H ₅₈ (406)	-	-	2.16
2-methyltetracosane	C ₂₅ H ₅₂ (352)	1.71	-	-
1-hexacosene	C ₂₆ H ₅₂ (364)	10.02	-	-
1,7-hexadecadiene	C ₁₆ H ₃₀ (222)	4.87	-	-

3.3. Prescription Medicine Bottles (MB) Pyrolysis

The Py-GC/MS experiment of MB was performed at 600 °C without a catalyst; the results are given in Table 4. The presence of a range of unsaturated compounds with one double bond can be observed. The most abundant compound found was 3-octadecene (C₁₈H₃₆), which accounted for 49% of the total area recorded from GC/MS. Additionally, 1-octene-3,7-dimethyl (8%), 3-tetradecene (5%), and 3-hexene (2.3%) were the major compounds present in the MB material. A few of the diene compounds included 1,13-tetradecadiene (1.5%), 1,19-eicosadiene (1%), and 1,4-undecadiene (1%). These results are consistent with the decomposition pattern of PP as per literature reports [30]. It has been reported that the noncatalytic degradation of PP under an inert atmosphere results in the formation of alkenes and α,ω -dienes mainly via dehydrogenation and fragmentation [30]. On the contrary, mainly aromatic compounds such as biphenyl (39%) and diphenylmethane (21%) were formed at 600 °C under catalytic pyrolysis (with Y-zeolite). Furthermore, aliphatic compounds such as octadecane-5-methyl (2.7%) and decane-2,3,5,8-tetramethyl (6.8%) with a low area percentage compared to aromatic ones were detected. These results indicate that Y-zeolite is not a very effective catalyst for the formation of saturated compounds from the catalytic pyrolysis of MB.

Table 4. Analysis of prescription medicine bottles using Py-GC/MS with and without Y-zeolite catalyst.

Compound Name	Formula (Molecular Weight, g/mol)	Area, %		
		Without Catalyst	With Y-Zeolite Catalyst	
		at 600 °C	at 600 °C	at 500 °C
Cyclopropane-butyl-	C ₇ H ₁₄ (98)	12.33	-	-
1-octene-3,7-dimethyl-	C ₁₀ H ₂₂ (140)	7.94	-	-
Pentane-2-cyclopropyl-	C ₈ H ₁₆ (112)	3.91	-	-
Cyclopentane-1,3-dimethyl-	C ₇ H ₁₄ (98)	1.35	-	-
1,5-hexadie-3-yne	C ₆ H ₆ (78)	0.70	-	-
3-hexene	C ₆ H ₁₂ (84)	2.28	2.88	-
4-undecene, 5-methyl-	C ₁₂ H ₂₄ (168)	-	0.74	9.65
1,5-decadiyne	C ₁₀ H ₁₄ (134)	0.82	-	-
2-nonyne	C ₉ H ₁₆ (124)	0.90	-	-

Table 4. Cont.

Compound Name	Formula (Molecular Weight, g/mol)	Area, %		
		Without Catalyst	With Y-Zeolite Catalyst	
		at 600 °C	at 600 °C	at 500 °C
1,1,4-trimethylcyclohexane	C ₉ H ₁₈ (126)	0.77	-	-
Cyclopentane-1,1,3,4-tetramethyl-	C ₉ H ₁₈ (126)	4.17	-	-
3-octyne-2-methyl-	C ₉ H ₁₆ (124)	0.86	-	-
1-hexene-3,3-dimethyl-	C ₈ H ₁₆ (112)	1.14	-	-
Octadecane-5-methyl-	C ₁₉ H ₄₀ (268)	-	2.66	-
Tritetracontane	C ₄₃ H ₈₈ (604)	-	1.33	21.37
1-nonene-4,6,8-trimethyl-	C ₁₂ H ₂₄ (168)	-	1.19	-
Benzene (1-methylpropyl)-	C ₁₀ H ₁₄ (134)	-	-	1.32
3-octadecene	C ₁₈ H ₃₆ (252)	48.57	-	-
1-octene-3,7-dimethyl-	C ₁₀ H ₂₀ (140)	-	1.15	-
Cyclopentane hexyl-	C ₁₁ H ₂₂ (154)	5.52	0.74	-
1,4-undecadiene	C ₁₁ H ₂₀ (152)	1.15	-	-
Benzene (1-cyclopropyl-1-methylethyl)-	C ₁₂ H ₁₆ (160)	-	1.06	-
Naphthalene	C ₁₀ H ₈ (128)	-	2.52	10.37
1,3-cyclopentadiene-5-(1,3-dimethylbutylidene)-	C ₁₁ H ₁₆ (148)	-	-	4.86
3-tetradecene	C ₁₄ H ₂₈ (196)	5.11	-	-
Decane-2,3,5,8-tetramethyl-	C ₁₄ H ₃₀ (198)	-	6.80	-
1,13-tetradecadiene	C ₁₄ H ₂₆ (194)	1.54	-	-
Biphenyl	C ₁₂ H ₁₀ (154)	-	39.15	6.27
2-allylnaphthalene	C ₁₃ H ₁₂ (168)	-	1.27	-
Acenaphthalene	C ₁₂ H ₁₀ (154)	-	0.42	-
Diphenylmethane	C ₁₃ H ₁₂ (168)	-	20.98	-
Benzene-1,1'-(1-methyl-1,2-ethanediyl) bis-	C ₁₅ H ₁₆ (196)	-	1.75	-
1,19-eicosadiene	C ₂₀ H ₂₈ (278)	0.94	-	-
1,1''-biphenyl-4-ethenyl-	C ₁₄ H ₁₂ (180)	-	7.51	-
Benzene-1,1'-(1,3-propanediyl) bis-	C ₁₅ H ₁₆ (196)	-	0.49	-
Diphenylacetylene	C ₁₄ H ₁₀ (178)	-	0.96	-
1,2-diphenylcyclopropane	C ₁₅ H ₁₄ (194)	-	0.16	-
Nonadecane	C ₁₉ H ₄₀ (268)	-	-	12.27
3-butyrylbenzene	C ₁₀ H ₁₀ (130)	-	2.92	4.87
1,3,5-cycloheptatriene-7,7-dimethyl-	C ₉ H ₁₂ (120)	-	0.61	-
Benzene-1,1''-(2-cyclopropen-1-ylidene) bis-	C ₁₅ H ₁₂ (192)	-	0.24	5.45
Anthracene	C ₁₄ H ₁₀ (178)	-	0.84	16.25
1,3-butadiene-1,4-diphenyl-	C ₁₆ H ₁₄ (206)	-	1.62	1.79
(4-methyl-1-methylenepent-4-enyl) benzene	C ₁₃ H ₁₆ (172)	-	-	5.52

There were differences in the area percentages among the products from the catalytic pyrolysis of MB with increasing pyrolysis temperature from 500 to 600 °C. At 500 °C, a single, exclusive aliphatic compound, i.e., nonadecane with a 12% area, was detected. Aromatic compounds such as anthracene (16%), naphthalene (10%), and biphenyl (6%) were also detected. On the contrary, with catalytic pyrolysis at a higher temperature of 600 °C, mainly aromatic compounds such as diphenylmethane and biphenyl were detected. These results indicated that Y-zeolite is only effective at a lower temperature, i.e., 500 °C, for the pyrolysis of MB plastic waste because of the presence of acid sites in the catalyst.

Proposed mechanism: The active intermediates involved during the pyrolysis (non-catalytic and catalytic) of PP/MB are depicted in Figure 3. Typically, the noncatalytic degradation of PP occurs via a free-radical process that includes initiation, propagation, and termination. The reaction mechanism showed a similarity with the PE degradation mechanism. In this mechanism, primary and secondary free radicals were formed after β -bond scission. Tertiary free radicals were produced by rearrangement reactions, and subsequent cracking led to the formation of alkenes and free radicals [43]. Moreover, a small secondary radical and a polymer chain with a terminal double bond were formed by β -scission on

the other side of the chain. The generated small secondary radicals were saturated through intramolecular hydrogen transfer, resulting in the formation of alkanes. The formation of 12% nonadecane at 500 °C occurred via intramolecular hydrogen transfer reactions. In our case, because of the low concentrations of saturated compounds/alkanes observed at 600 °C, transfer reactions appeared to contribute a minor role in MB degradation.

Another mechanism reported in the literature for PE/PP degradation was ionic degradation [43,44]. This mechanism involves two steps: (i) abstraction of a hydride ion (due to the catalytic Lewis acid sites) from the polymer chain or addition of a proton (because of the catalytic Brønsted acid sites) to the unsaturated sites (alkenes) formed by thermal degradation, and (ii) isomerization of the secondary and tertiary ions and β -scission. This ionic mechanism might have been the reason for the formation of cyclic and aromatic compounds during the catalytic pyrolysis at temperatures of 500 and 600 °C.

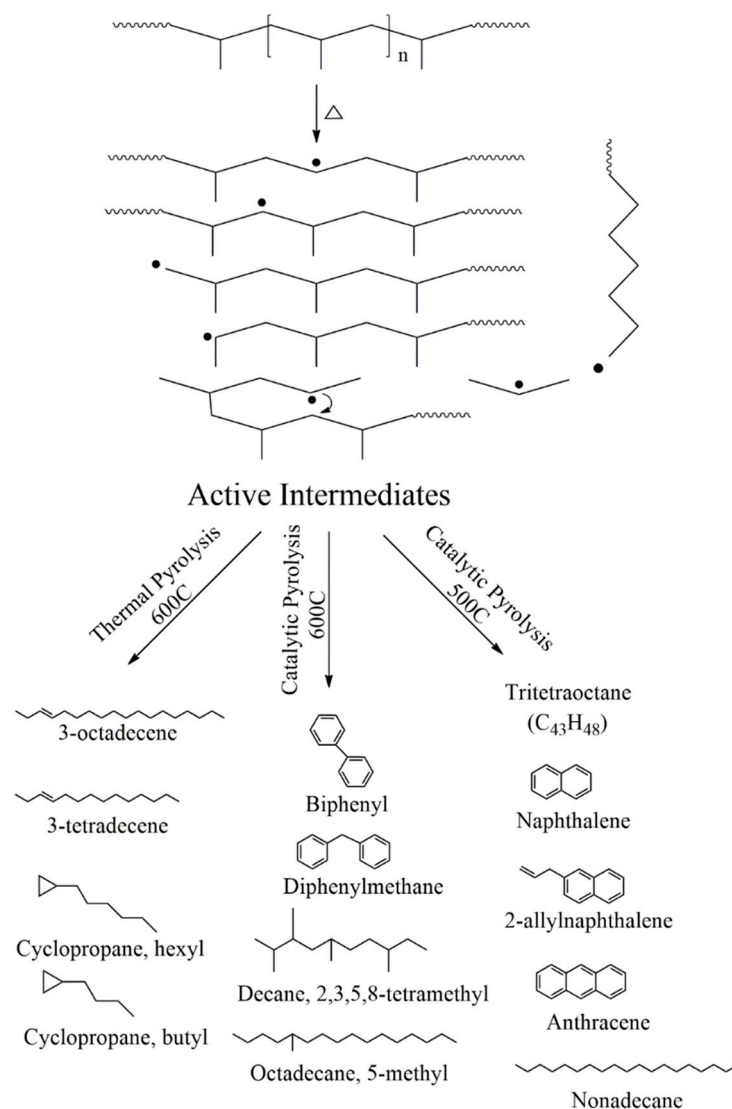


Figure 3. Reaction mechanism for the noncatalytic and catalytic pyrolysis of polypropylene present in prescription medicine bottles [45,46].

3.4. Packaging Materials (PM) Pyrolysis

The Py-GC/MS data presented in Table 5 show the product distribution obtained after pyrolysis of PM. The predominant noncatalytic degradation products at 600 °C with PM were styrene (48%) and toluene (22%), followed by the styrene dimer, bibenzyl (14%). As per the literature reports, pyrolysis of neat polystyrene (PS) yielded mainly styrene monomers

and oligomers (dimers and trimers) [30,32]. Therefore, PM plastic waste contained PS. The catalytic pyrolysis of PM material was conducted in the presence of an FCC spent catalyst. In comparing the reaction at 600 °C with and without a catalyst, it was observed that the catalyst played a decisive role in the formation of aliphatic and olefinic compounds. The results indicated that, when the catalytic pyrolysis of PM material was carried out at 500 and 600 °C, toluene completely disappeared, and the amount of styrene decreased, but new branched aliphatic and olefinic compounds were formed.

Table 5. Analysis of packaging materials by Py-GC/MS with and without FCC spent catalyst.

Compound Name	Formula (Molecular Weight, g/mol)	Area, %		
		Without Catalyst	With FCC Spent Catalyst	
		at 600 °C	at 600 °C	at 500 °C
n-hexane	C ₆ H ₁₄ (80)	-	-	1.15
Pentane-2,3-dimethyl-	C ₇ H ₁₆ (100)	-	14.31	9.01
Toluene	C ₇ H ₈ (92)	21.45	-	-
Styrene	C ₈ H ₈ (104)	48.35	22.47	36.48
α-methylstyrene	C ₉ H ₁₀ (118)	-	-	18.58
2,4-heptadiene	C ₇ H ₁₂ (96)	-	15.30	-
1,6-heptadiyne	C ₇ H ₈ (92)	-	-	1.44
3-undecen-1-yne	C ₁₁ H ₁₈ (150)	-	1.10	-
Cyclopentane-1-ethyl-2-methyl-cis	C ₈ H ₁₆ (112)	-	6.62	-
1-decyne	C ₁₀ H ₁₈ (138)	-	5.77	-
3-hexene-2,2,5,5-tetramethyl-	C ₁₀ H ₂₀ (140)	-	4.98	-
Cyclohexane-1,2,4-trimethyl-	C ₉ H ₁₈ (126)	-	2.13	-
Octane-2,7-dimethyl-	C ₁₀ H ₂₂ (142)	-	3.33	-
Cyclopentane-1,2-dipropyl-	C ₁₁ H ₂₂ (154)	-	0.83	-
4-tetradecene	C ₁₄ H ₂₈ (196)	-	5.66	-
Biphenyl	C ₁₂ H ₁₀ (154)	-	-	2.26
2-undecene	C ₁₁ H ₂₂ (154)	-	-	0.63
2,3,5,8-tetramethyldecane	C ₁₄ H ₃₀ (198)	-	-	0.61
Acenaphthalene	C ₁₂ H ₁₀ (154)	-	-	0.64
Biphenylene	C ₁₂ H ₈ (152)	-	-	2.38
Tritetracontane	C ₄₃ H ₈₈ (604)	-	1.92	-
Cyclotetradecane	C ₁₄ H ₂₈ (196)	-	-	2.32
Decane-3-methyl-	C ₁₁ H ₂₄ (156)	-	-	6.05
Bibenzyl	C ₁₄ H ₁₄ (182)	14.09	-	-
Decane-2,6,10-trimethyl	C ₁₅ H ₃₂ (212)	-	-	17.73
Decane-2,3,5,8-tetramethyl-	C ₁₄ H ₃₀ (198)	-	6.70	-
Dodecane-2-phenyl-	C ₁₈ H ₃₀ (246)	-	-	0.73
Naphthalene-1,2,3,4-tetrahydro-2-phenyl-	C ₁₆ H ₁₆ (208)	16.11	-	-
Bicyclo [10.1.0] tridec-1-ene	C ₁₃ H ₂₂ (178)	-	8.88	-

When the reaction temperature was increased from 500 to 600 °C, the styrene amount decreased to 22%, and aliphatic branched hydrocarbons such as pentane-2,3-dimethyl (14%) and decane-2,3,5,8-tetramethyl (6.7%) were detected. In addition, olefinic compounds such as 4-tetradecene (5.7%), 1-decyne (5.8%), 3-undecen-1-yne (1.1%), and branched cyclic compounds (9.6%, total) were detected in abundance. At 600 °C, the catalyst was able to actively break the benzene ring in styrene and toluene to form aliphatic and olefinic compounds. The product composition indicated that the FCC spent catalyst was effective in increasing the cracking activities of PM plastic waste.

Proposed mechanism: Both end-chain and random-chain scissions that form free radicals were found to be responsible for the degradation of PS via the pyrolysis process (reaction mechanism shown in Figure 4). The depolymerization of radicals formed by random thermal cleavage of the main chain led to the formation of styrene [42,47]. However, the styrene dimer was formed by an intermolecular transfer between radicals [47]. The molecular weight of the polymeric chain was reduced by intermolecular transfer reactions, resulting in the production of short-chain fragments. PS was found to be suitable for

monomer (feedstock) recovery in high yields, and product composition was strongly dependent on the plastic types [42].

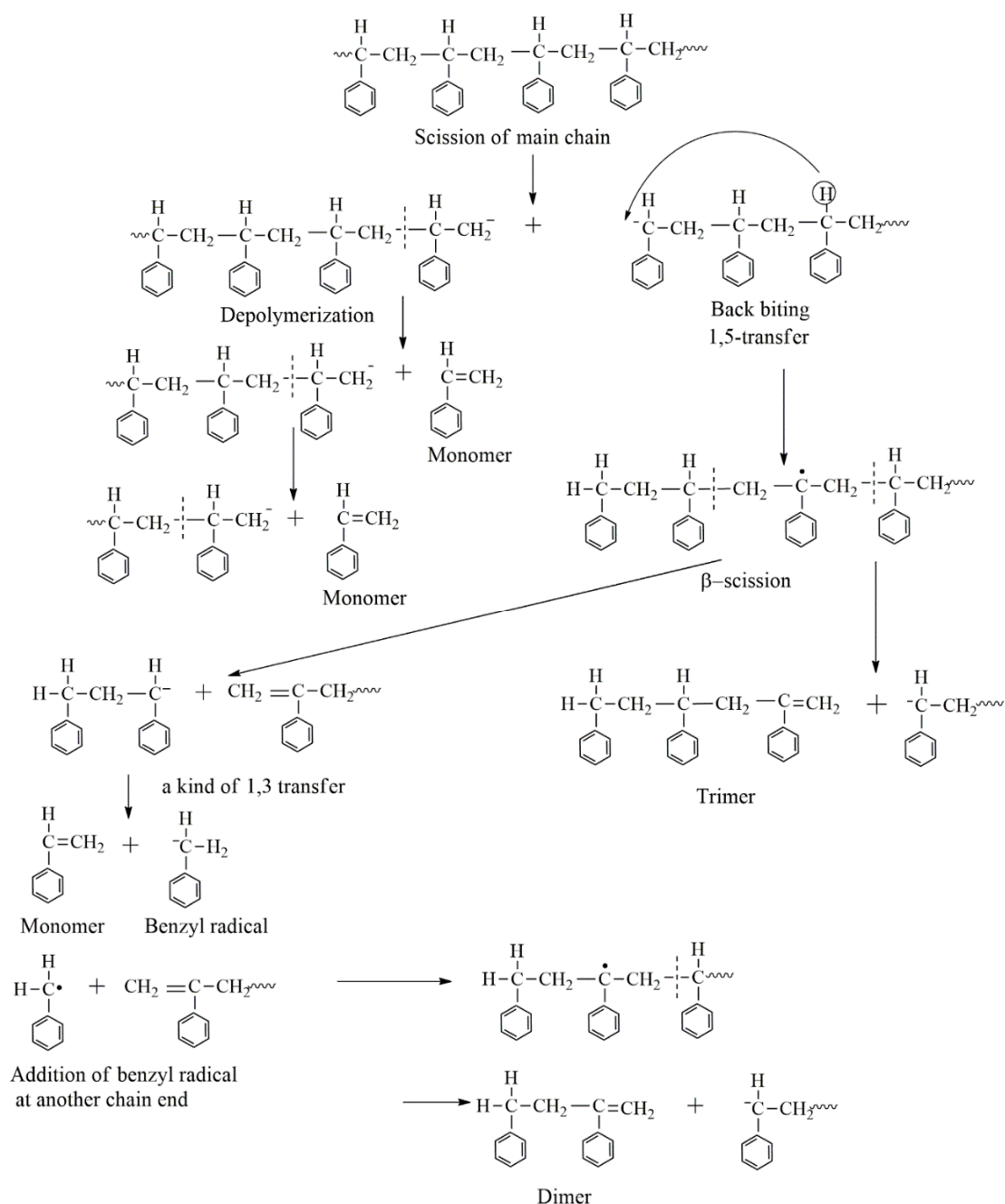


Figure 4. Reaction mechanism for the noncatalytic pyrolysis of polystyrene polymers [31]. (Adapted with permission from Ref. [31], 2000, John Wiley and Sons).

In the present work, during the noncatalytic pyrolysis of PM styrene, dimers and trimers were the major products. On the other hand, significant quantities of olefinic and aliphatic saturated compounds were formed in the presence of the catalyst. This occurred due to the presence of acid sites in the catalyst used. Moreover, the yield of some cyclic compounds was also detected, suggesting that cyclization reactions might have occurred due to the large surface area available for the long-chain reactive species. The detailed mechanism for the catalytic degradation of PM is depicted in Figure 5a,b. The major routes for the generation of styrene and dimers are depicted. Tertiary carbocations were produced at a higher temperature, and then underwent successive β -scission and H-shift

reactions to produce aromatic compounds in low quantities compared to noncatalytic degradation [45,46,48]. β -scission occurred at the specific chain-end positions, resulting in the formation of free-radical intermediates and stable olefinic end groups. These free-radical intermediates could either undergo β -scission or abstract a proton from another chain and stabilize to form aliphatic saturated compounds. Saturated aliphatic and olefinic compounds could also be formed from the side-chains present in the main polymer chains of the plastic waste PM, as presented in Figure 5b.

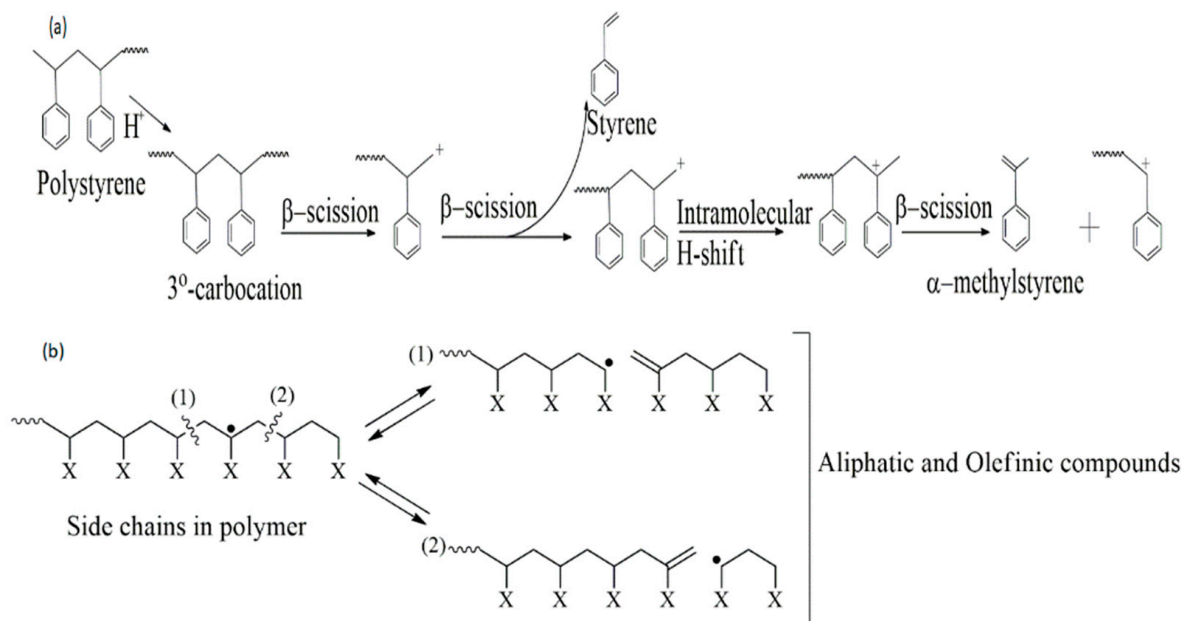


Figure 5. Proposed reaction mechanism for the products formed from (a) noncatalytic and (b) catalytic pyrolysis of polystyrene present in packaging material [48]. (Adapted with permission from Ref. [48], 1998, John Wiley and Sons).

3.5. Industrial Plastic Waste 2 (IPW2) Pyrolysis

The product composition from the pyrolysis of IPW2 is reported in Table 6. The catalyst used for the pyrolysis of IPW2 was sulfated zirconia. In the case of the noncatalytic pyrolysis of IPW2 materials at 600 °C, 42% 2-heptenoic acid tetradecyl ester and 40% dimethyl-4-methylphthalate were the major compounds detected. Low amounts of alkenes (5.8% 2-decene, 4.1% 1-octene-6-methyl-, and 2% 1-tridecene) were also formed. The product distribution after the noncatalytic degradation of IPW2 suggests that this plastic waste material resembled a polyurethane (PU) polymer. The amount of these major compounds detected in noncatalytic pyrolysis decreased with a sulfated zirconia catalyst at 500 °C and 600 °C temperatures. The lowest amounts of 2-heptenoic acid tetradecyl ester (15%) and dimethyl-4-methylphthalate (6%) were detected at 600 °C. Furthermore, catalytic pyrolysis with a sulfated zirconia catalyst at 600 °C produced various alkenes and cycloalkanes. For instance, alkenes such as 3-heptene-4-propyl (18%), 1-octene-6-methyl (15%), 2-decene (9%), and 5-undecene-4-methyl (5%), and cycloalkanes such as cyclopentane butyl (12%), cyclooctane methyl (4.7%), and cyclooctane butyl (3%) were observed. When the catalytic pyrolysis was conducted at 500 °C, similar alkenes and cycloalkanes were present; however, their area percentage were lower compared to that observed at 600 °C. Catalytic pyrolysis at 500 °C led to the production of alkenes such as 1-octene-6-methyl (8.2%), 3-heptene-4-propyl- (23%), and 2-decene (4%), and cycloalkanes such as cyclopentane-3-butyl (8%) and cyclohexane-1,3,5-trimethyl- (3%). These results indicated that the sulfated zirconia was effective as a catalyst for PU pyrolysis. It was also observed that approximately 40–45% of the sample was found as residue in the quartz tube after the Py-GC/MS experiment. These results are consistent with the results from the TGA study [14] due to the presence of

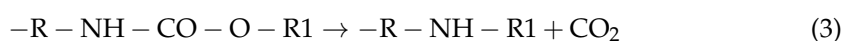
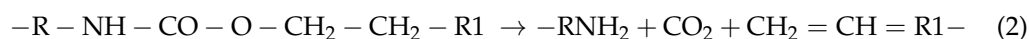
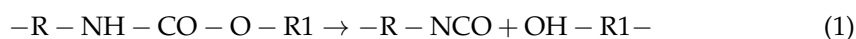
extraneous materials (mainly fillers or other additives) typically present in these industrial plastic wastes. These additives might have affected the pyrolysis process.

Table 6. Analysis of industrial plastic waste 2 by Py-GC/MS with and without sulfated zirconia catalyst.

Compound Name	Formula (Molecular Weight, g/mol)	Area, %		
		Without Catalyst	With Sulfated Zirconia Catalyst	
		at 600 °C	at 600 °C	at 500 °C
Cyclopentane-butyl-	C ₉ H ₁₈ (126)	-	11.62	7.99
1-octene-6-methyl-	C ₉ H ₁₈ (126)	4.13	14.73	8.23
4-nonene	C ₉ H ₁₈ (126)	-	-	2.36
5-undecene-4-methyl-	C ₁₂ H ₂₄ (168)	0.98	5.12	2.05
Cyclooctane-methyl-	C ₉ H ₁₈ (126)	-	4.73	-
Cyclohexane-1,3,5-trimethyl-	C ₉ H ₁₈ (126)	-	-	3.16
3-heptene-2-methyl-	C ₈ H ₁₆ (112)	-	2.86	2.23
3-heptene-4-propyl-	C ₁₀ H ₂₀ (140)	-	18.17	22.86
2-decene	C ₁₀ H ₂₀ (140)	5.81	9.03	3.93
Cyclooctane-butyl-	C ₉ H ₁₈ (126)	-	3.01	0.79
2-octenal	C ₈ H ₁₄ O (126)	-	0.83	-
1-tetradecene	C ₁₄ H ₂₈ (182)	-	1.62	-
1-tridecene	C ₁₃ H ₂₆ (182)	2.04	-	1.35
Phthalic anhydride	C ₈ H ₄ O ₃ (148)	-	4.24	2.70
n-heptyl isocyanate	C ₈ H ₁₅ NO (141)	-	2.02	1.22
1-methylpentyl cyclopropane	C ₉ H ₁₈ (126)	2.76	-	-
Biphenyl	C ₁₂ H ₁₀ (152)	-	-	0.58
Cyclododecane	C ₁₂ H ₂₄ (168)	-	-	0.30
Decane-2,3,5,8-tetramethyl-	C ₁₄ H ₃₀ (198)	-	0.22	0.32
Biphenylene	C ₁₂ H ₈ (152)	-	-	0.70
Tritetracontane	C ₄₃ H ₈₈ (604)	0.30	-	-
Bibenzyl	C ₁₄ H ₁₄ (182)	0.21	-	-
Cyclotetradecane	C ₁₄ H ₂₈ (196)	0.18	0.13	-
Decane-2,3,5,8-tetramethyl-	C ₁₄ H ₃₀ (198)	0.42	-	-
3-butylbenzyl	C ₁₀ H ₁₀ (130)	0.23	-	-
Anthracene	C ₁₄ H ₁₀ (178)	-	0.09	-
3-eicosene	C ₂₀ H ₄₀ (280)	0.09	-	-
Tetradecanoic acid-12-methylmethylester	C ₁₆ H ₃₂ O ₂ (256)	-	-	-
1-tetracosene	C ₂₄ H ₄₈ (336)	0.16	0.13	0.19
Naphthalene-2-phenyl-	C ₁₆ H ₁₂ (204)	-	-	0.19
1-nonadecene	C ₁₉ H ₃₈ (266)	0.50	0.09	-
1,9-eicosadiene	C ₂₀ H ₃₈ (278)	0.27	-	-
1-benzylindole	C ₁₅ H ₁₃ N (207)	-	-	-
2-heptenoic acid tetradecyl ester	C ₂₂ H ₄₂ O ₂ (324)	42.18	-	11.51
Dimethyl-4-methylphthalate	C ₂₆ H ₂₄ O ₄ (418)	39.72	-	27.08

Proposed mechanism: Polyurethane (PU) contains a base resin and a catalyst as two major components. Typically, the base resin includes polyols such as low-molecular-weight esters, and the catalyst includes polyisocyanates such as toluene diisocyanate, diphenylmethane p,p'-diisocyanate, isophorone diisocyanate, and hexamethylene diisocyanate. In general, the degradation of urethane linkage occurs through three pathways:

- Dissociation of urethane to isocyanate (R–NCO) and alcohol (OH–R1–),
- Dissociation to primary amine (R–NH₂), olefin (CH₂=CH–R1–), and carbon dioxide,
- Formation of a secondary amine (–R–NH–R1) via the removal of carbon dioxide (CO₂) [34–36].



Detailed information on the degradation mechanism for the IPW2-PU catalytic pyrolysis is presented in Figure 6. In the present work, the most abundant compound reported from the noncatalytic pyrolysis of IPW2-PU was 2-heptenoic acid tetradecyl ester, which was formed from the degradation of the polyester construction of PU. The *n*-heptyl isocyanate volatilized at the initial step, and then the urethane bond groups of polymeric chains broke up into isocyanates and polyols as per Equation (1). The resulting isocyanates formed from decomposition could not volatilize and might have been trapped as residues in the quartz tube. However, in the presence of a sulfated zirconia catalyst, polyol components started to decompose into esters, olefins, and cycloalkanes in the presence of a catalyst [49]. As reported in the pyrolysis study of PU foams, diols formed as per Equation (1) underwent dehydration to produce secondary products with double bonds as the end groups [50–53]. In our case, secondary amine products were not detected (Table 6). The results suggest that sulfated zirconia was a good catalyst for the pyrolysis of the polyester chain of PU foam plastic materials.

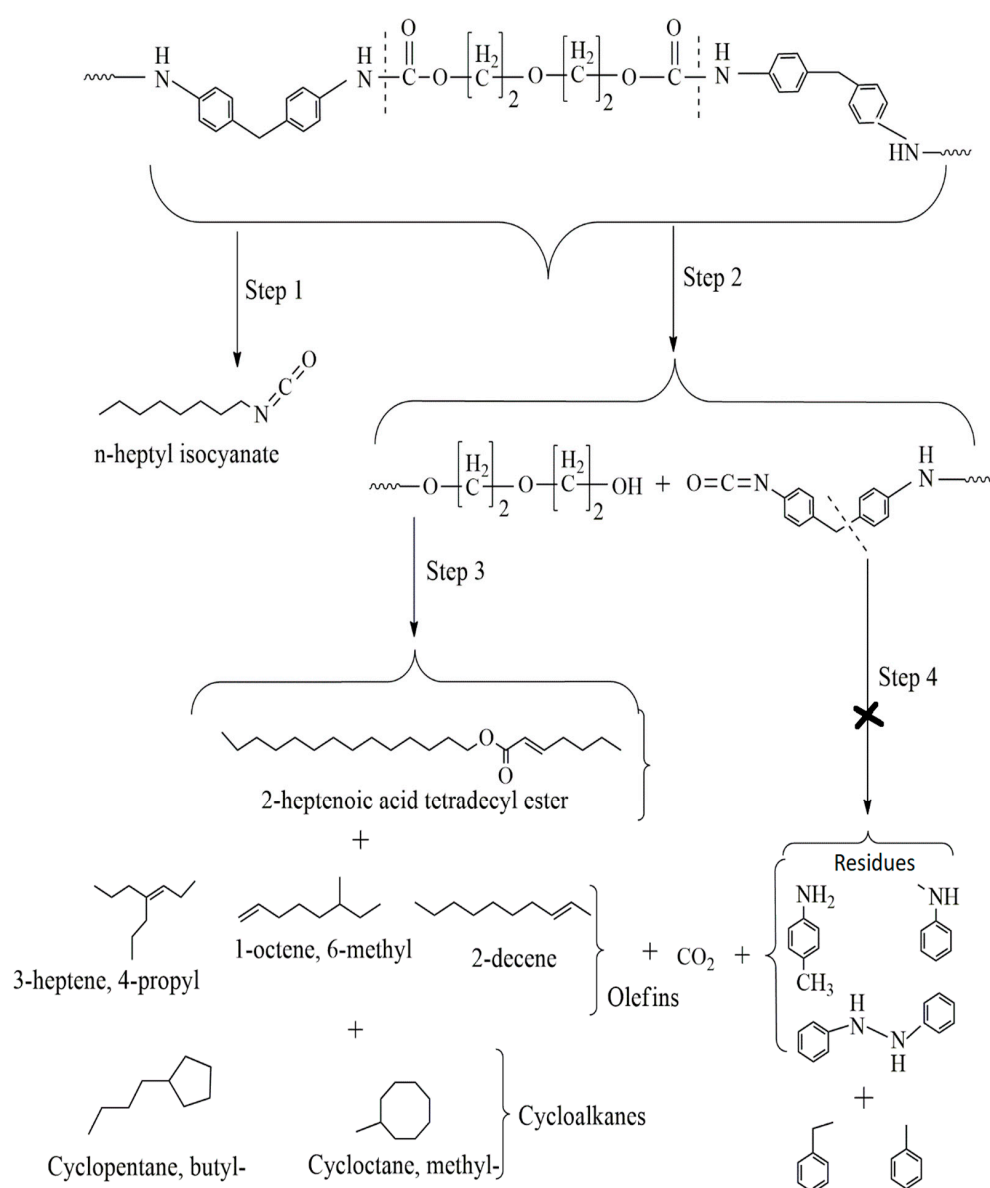


Figure 6. Reaction mechanism for the noncatalytic (Step 1) and catalytic (Step 2) pyrolysis of polyurethane present in industrial plastic waste 2 [52]. (Adapted with permission from Ref. [52], 2013, Elsevier).

4. Batch-Scale Pyrolysis Validation of Landfill Liner (LL) Plastic Waste

PCO-LL and its distilled fractions were analyzed for elemental composition, and the results are reported in Table 7. The calorific value and elemental composition for commercial jet fuel are also given in Table 7 for comparison. The results show that the PCO and the distillate fractions, except the gasoline range fraction (from the PCO), did not contain oxygen. In contrast, 4.6 wt.% oxygen was present in the gasoline range fraction. The elemental composition and calculated HHV of the jet fuel fraction obtained from PCO-LL were quite similar to commercial jet fuel.

Table 7. Elemental properties of landfill liner plastic waste and its pyrolyzed products.

Samples	Elemental Properties				Calorific Value
	Carbon, wt.%	Hydrogen, wt.%	Nitrogen, wt.%	Oxygen, wt.%	HHV, MJ/kg
Landfill liner (LL)	84.2	14.0	0.4	1.40	48.3
Plastic crude oil (PCO)	85.9	13.9	0.2	-	48.8
Distillate Fractions					
Gasoline range (<150 °C)	82.0	13.3	0.1	4.60	46.1
Aviation range fuel (150–275 °C)	85.8	14.3	0.2	-	49.4
Gas oil plus range (>275 °C)	86.1	14.1	0.3	-	49.2
Commercial jet fuel	86.0	13.9	0.2	-	48.9

4.1. Compositional Analysis of PCO Distillate Fractions

A detailed compositional analysis of distillate fractions obtained from PCO-LL, recovered after batch pyrolysis of LL plastic waste, was carried out using FT-IR and ^1H -NMR spectroscopy. Figure 7 presents the FT-IR spectra. The bands in the region $3000\text{--}2800\text{ cm}^{-1}$ showed the presence of $-\text{CH}_3$, $-\text{CH}_2$, and $-\text{CH}$ groups of saturated components present in samples. Major peaks at 1450 and 1375 cm^{-1} were due to the asymmetric and symmetric deformation stretching of $-\text{CH}_3$ groups. The presence of $\text{C}=\text{C}$ stretching vibrations ($1640\text{--}1650\text{ cm}^{-1}$) indicated the presence of alkenes, albeit with lower concentrations. The high intensity of peaks at $2800\text{--}3000$ and $1320\text{--}1480\text{ cm}^{-1}$ suggested the presence of a higher concentration of alkanes. The bands in the region between 1575 and 1675 cm^{-1} and similarly between 875 and 950 cm^{-1} represented the $\text{C}=\text{C}$ stretches. Two peaks, i.e., at 990 and 910 cm^{-1} , in all spectra were due to the presence of monosubstituted double bond. The peak near 720 cm^{-1} was due to the cis di-substituted double bond. Similar characteristics were reported in the literature [7,33,54]. In Figure 7d, the FT-IR spectrum of the aviation range fuel fraction obtained from PCO-LL is compared with a commercially available jet fuel. It can be observed that the spectra were almost similar except in the $900\text{--}1000\text{ cm}^{-1}$ region.

^1H -NMR spectroscopy was performed for the quantification of hydrocarbons, and the results are presented in Table 8. ^1H -NMR spectra are presented in the Supplementary Materials (Figure S1). Paraffin and olefin concentrations of the distillate fractions of PCO-LL were found in the range of $81\text{--}99\%$ and $1\text{--}9\%$, respectively. The olefinic proton concentration was high in the gasoline range fraction, resulting in a lower paraffinic proton concentration. The aviation range fuel fraction from PCO-LL contained 95.5% paraffinic protons, 4.2% olefinic protons, and 0.3% aromatic protons. The paraffinic protons were almost identical to commercial jet fuel while the olefinic protons were higher compared to the commercial jet fuel, and the aromatic protons were lower compared to the commercial jet fuel. Due to the low aromaticity of the aviation range fuel fraction, this fraction either has to be supplemented by the addition of monoaromatics or has to be blended with commercial jet fuel to meet the aromatic requirement. According to the Py-GC/MS results, landfill liner plastic waste resembled PE polymer. Pinto et al. [55] reported that PP and PE undergo random scission and generate free radicals at high temperatures. The radicals then undergo β -scission to produce monomers which are stabilized by intramolecular or intermolecular hydrogen transfer. The successive β -scission reaction of the secondary radicals limits the formation of dienes and olefins. On the contrary, paraffins are formed

by intermolecular hydrogen transfer. At high temperatures, the possibility of successive scission with intramolecular hydrogen transfer is predicted because of the many hydrogen atoms in the radical chain.

Table 8. Hydrogen distribution of the distillate fraction of plastic crude oil obtained after pyrolysis of landfill liner plastic waste (PCO-LL).

Distillate Fractions	Hydrocarbon Composition, wt. %		
	Paraffinic Hydrogen	Olefinic Hydrogen	Aromatic Hydrogen
Gasoline range (<150 °C)	90.9	8.7	0.4
Aviation range fuel (150–275 °C)	95.5	4.2	0.3
Gas oil plus range (>275 °C)	98.6	1	0.4
Commercial jet fuel	95.2	1.3	3.5

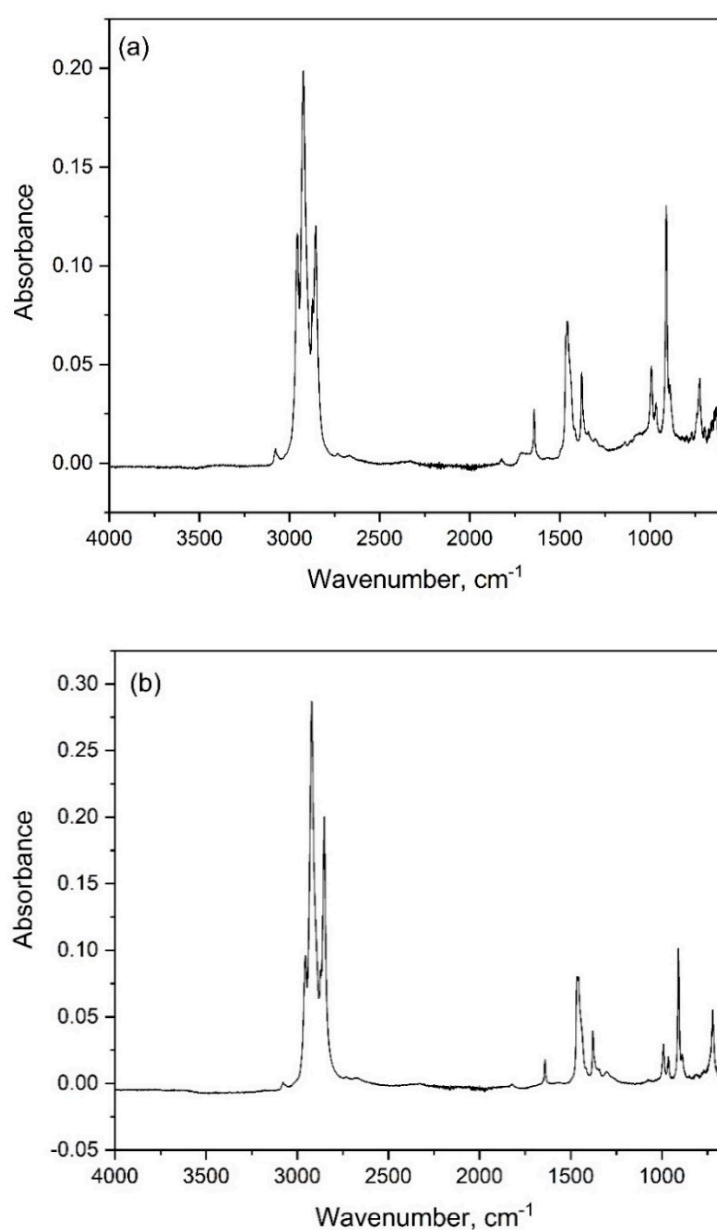


Figure 7. Cont.

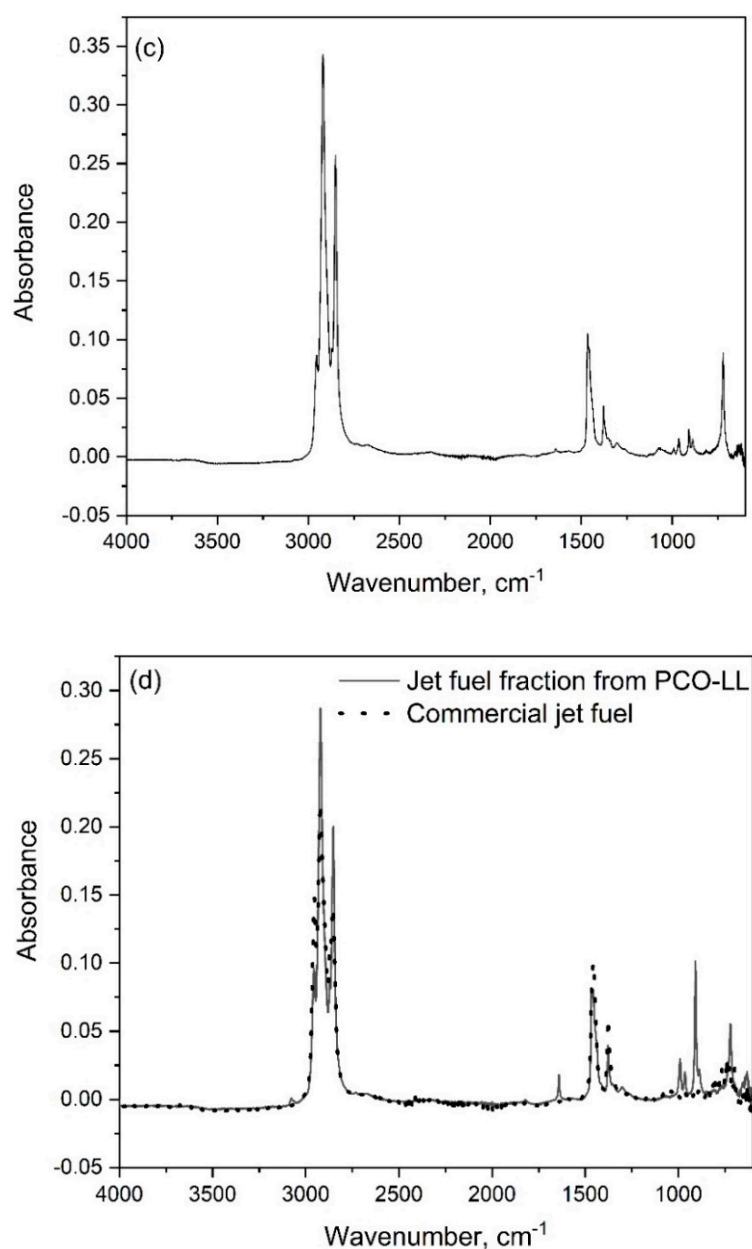


Figure 7. FT-IR spectra of the distillate fractions of plastic crude oil obtained after pyrolysis of landfill liner plastic waste (PCO-LL): (a) gasoline range, (b) aviation range fuel, (c) gas oil plus range, and (d) comparison of aviation range fuel fraction (from PCO-LL) with commercial jet fuel.

The distillate fractions were also characterized by GC, and the results are given in Table 9. In the aviation range fuel fraction, the saturated hydrocarbons in the carbon number range C_{11} – C_{16} were found to be in significant quantities, along with the unsaturated hydrocarbons. The unsaturated compounds were mainly generated due to the random scission degradation mechanism of plastic followed by stabilization of the intermediate radicals.

4.2. Fuel Properties of Jet Fuel Fraction

The LL plastic waste was mainly composed of carbon and hydrogen. Therefore, the properties obtained from LL-based fuels were like hydrocarbon fuels. The aviation range fuel fraction produced from the pyrolysis of the LL plastic waste was further analyzed for the fuel properties (determined using ASTM, EN, and AOCS methods) and was compared with the commercial jet fuel. The results are shown in Table 10. The aviation range fuel fraction from the PCO obtained through pyrolysis of landfill liner plastic waste exhibited

characteristics of commercial jet fuel. On comparing the properties of aviation range fuel fraction with commercial jet fuel, it was found that an improvement in low-temperature flow properties (pour point -15°C and cloud point -17.2°C) is needed, which can be achieved through isomerization, while oxidation stability can be improved through hydrogenation to reduce olefins. The viscosity was slightly higher (1.88 cSt at 40°C) compared to the commercial jet fuel (1.31 cSt at 40°C) and could be adjusted by changing the upper boiling range to a lower temperature. The HHV determined using a bomb calorimeter was comparable to that of commercial jet fuel. Overall, the aviation range fuel fraction showed similar energy content and surface tension, but low viscosity, poor low-temperature flow properties, and low oxidation stability. These data suggest that there is potential for coprocessing plastic crude oil with petroleum crude oil in refineries to produce commercially available fuels for direct applications.

Table 9. Gas chromatographic analysis of the distillate fraction of plastic crude oil obtained after pyrolysis of landfill liner plastic waste (PCO-LL).

Compound Name	Area, %
Gasoline range fraction ($<150^{\circ}\text{C}$)	
1-hexene	7.7
1-heptene	10.3
Heptane	11.0
cis-1-butyl-2-methylcyclopropane/1-cotene	12.6
Heptane, 2,4-dimethyl-	13.1
1-nonene	13.2
Nonane	13.0
1-decene	11.2
Decane	8.0
Aviation range fuel fraction ($150\text{--}275^{\circ}\text{C}$)	
1-undecene	4.9
Undecane	5.1
1-dodecene	7.3
Dodecane	7.2
1-tridecene	7.5
Tridecane	7.8
1-tetradecene	8.0
Tetradecane	9.1
1-pentadecene	7.3
Pentadecane	11.3
1-hexadecene	5.6
Hexadecane	11.5
Gas oil plus range fraction ($>275^{\circ}\text{C}$)	
Heptadecane	7.2
Heptadecane	8.4
Octadecane	15.5
Nonadecane	18.9
Eicosane	17.7
Heneicosane	15.2
Octacosane	11.0
Hentriacontane	8.1
Tetracosane	5.0

The product yields and quality (fuel properties) depend on the plastic waste feedstocks and the reaction parameters. The literature reports related to the utilization of real plastic feedstocks are very few. In our earlier publication [14], we conducted batch pyrolysis of prescription medicine bottles (MBs). The results showed that the catalysts lowered the pyrolysis temperature and improved the selectivity of the motor gasoline. The produced fuel was of better quality. Kizza et al. [56] conducted a comparison between plastic-derived fuel oil and conventional diesel based on qualitative analysis and energy recovery potential. The results showed that there were not many differences between the densities

and water contents of fuel oils. The values of the pour point and viscosities were within the recommended range. Energy recovery calculations revealed that plastic-derived fuel oil has the potential to produce energy equivalent to 203,000 barrels of oil. The authors concluded that the plastic-derived fuel oil is a potential substitute for conventional diesel oil.

Table 10. Fuel properties of aviation range fuel fraction from PCO-LL and commercial jet fuel.

Properties	Method Used	Aviation Fuel Range Fraction	Commercial Jet Fuel
Cloud point, °C	ASTM D5773	-17.2 ± 0.7	-54.8 ± 0.2
Pour point, °C	ASTM D5949	−15	−65
Cold filter plugging point, °C	ASTM D6371	−19	>51
Induction period, h	EN 15751	16.3 ± 0.1	>90
Kinematic viscosity at 40 °C, cSt	ASTM D445	1.88	1.31
Kinematic viscosity at −20 °C, cSt	ASTM D445	−	4.16 ± 0.01
Oxidative stability, °C		201.5 ± 0.6	217 ± 0.3
Specific gravity, 15 °C	ASTM D 4052	0.7933	0.8126
Density at 15 °C, kg/m ³	ASTM D4052	0.7925	0.8118
Acid value, mg KOH/g	AOCS Cd 3d-63	0.24 ± 0.02	0.02 ± 0.01
Gross Heat of Combustion (higher heating value, MJ/kg)	ASTM D4809	45.757 ± 0.255	45.17 ± 0.114
Surface tension at 25 °C, mN/m		25.6 ± 0.0	24.8 ± 0.1
Surface tension at 40 °C, mN/m		24.2 ± 0.1	23.2 ± 0.1

5. Discussion

The plastic pyrolysis process involves controlled heating of the material in the absence of oxygen, resulting in the breakdown of the large macromolecular structures of polymers into smaller oligomer and monomer molecules. The degradation of the molecules depends on reaction conditions such as temperature, residence time, and the presence of catalysts. The pyrolysis products also relate directly to the chemical structure and mechanism of decomposition. The chemical identification of plastic waste is necessary to develop an effective process for the pyrolysis of plastic waste at a large scale. The Py-GC/MS technique is well proven and effective in investigating the production of main compounds from the pyrolysis of virgin plastics. This technique provides a quick and easy way to determine the degradation products. In addition, Py-GC/MS is a convenient and robust technique to analyze the whole plastic waste, thus also enabling the identification of other chemical impurities in the plastic waste. In the case of catalytic pyrolysis, Py-GC/MS provides information about the cracking efficiency of the catalysts. The degradation product composition obtained from the Py-GC/MS technique helps to deduce the reaction mechanism involved during the pyrolysis process. This in turn helps to design new catalysts for the process. Therefore, in the present work, Py-GC/MS experiments were performed on the five different types of post-consumer plastic wastes such as packaging materials, landfill liners, medicine bottles, and two different industrial plastic wastes (IPW1 and IPW2) at 600 °C with 5 min reaction time. Both noncatalytic and catalytic pyrolysis processes of all the plastic wastes used were studied, and the reaction mechanisms involved in both processes were described. A summary of the product distribution from the studied five different plastic wastes is presented in Figure 8. Pyrolytic depolymerization of polyolefin generates a wide range of hydrocarbons through a random-chain scission reaction mechanism. The noncatalytic degradation products detected from LL and IPW1 plastic wastes showed a resemblance to polyethylene. Polyethylene mainly contains secondary carbon in its linear straight-chain structure; thus, there are fair probabilities of random cracking during pyrolysis. However, the products formed were different in different plastic wastes; for example, mainly aromatic compounds were detected in the noncatalytic pyrolysis of LL, while alkenes, alkynes, cycloalkanes, and alkanes were seen in the noncatalytic pyrolysis of IPW1. These results indicated that LL contains impurities or additives that are responsible for the different product compositions under same reaction conditions. It has been observed that the catalytic pyrolysis temperature affects the degradation products; for example, aro-

matic compounds were predominant at a lower temperature, while saturated compounds were in excess at a higher temperature. The stable tertiary carbon present in MB waste plastic had a higher number of small, cracked molecules than polyethylene. The pyrolysis of MB showed a resemblance to polypropylene because of the presence of alkenes and α , ω -dienes in the Py-GC/MS chromatogram, whereas, in catalytic pyrolysis, mainly aromatic compounds were observed due to the ionic degradation mechanism involved during the catalytic pyrolysis [49,51]. The higher yield of styrene dimer in noncatalytic pyrolysis of PM was mainly due to intramolecular radical transfer reaction. The Py-GC/MS results from the PM showed the presence of polystyrene as a major polymer, and the FCC spent catalyst was observed to play an important role in the formation of aliphatic and olefinic compounds. These results are consistent with the reported pyrolysis of virgin PS [57–60]. IPW2 showed a resemblance to the polyurethane foams, and the sulfated zirconia used as a catalyst for catalytic pyrolysis was found to be effective in producing esters, olefins, and cycloalkanes from IPW2. About 50–55% of this plastic waste was pyrolyzed, while the remaining 40–45% was found as residue in the quartz tube after the Py-GC/MS experiment. This could be due to the presence of inert filler material, additives, and/or incomplete depolymerization under current pyrolysis conditions.

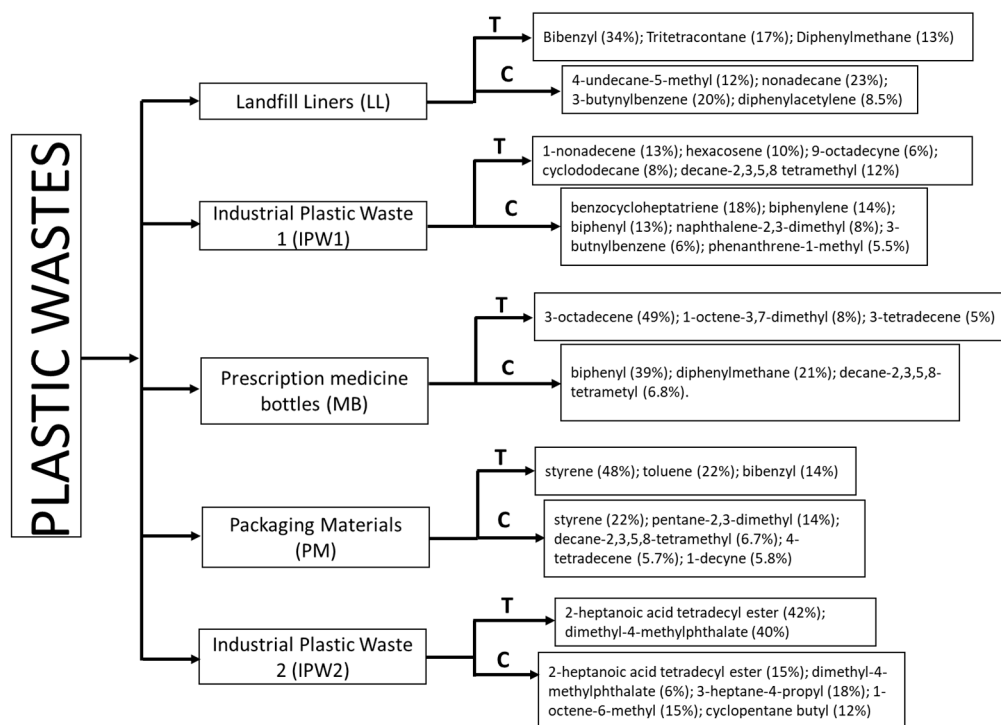


Figure 8. Summary of product distribution from five different plastic wastes using pyrolysis-GC/MS experiments at 600 °C temperature (T = thermal or non-catalytic pyrolysis, C = catalytic pyrolysis); only products with more than 5% chromatographic area are shown.

The results demonstrated the usefulness and effectiveness of the Py-GC/MS technique. The results confirmed the high sensitivity of the technique to detect and identify the polymers present in the plastic waste and impurities, providing information that can help to design the pyrolysis process at a large scale. The varying composition of products from the same kind of polymer, but different post-consumer plastic waste might be due to the variation in molecular weight and amorphous/crystalline ratio, presence of inert/organic filler, and interaction of the different impurities or additives present in waste feeds. Overall, it was observed that the addition of a catalyst to the plastic wastes resulted in different product compositions and could be used to increase the selectivity of specific compounds in the process. According to the information collected from the pyrolysis of plastic wastes

by Py-GC/MS experiments, process parameters including screening/selection of catalysts can be optimized to design the pyrolysis process to produce desired fuels and chemicals.

6. Conclusions

This study showed the practicality and effectiveness of the Py-GC/MS technique in demonstrating the noncatalytic and catalytic degradation mechanisms involved during the pyrolysis of postconsumer polyolefin, polystyrene, and polyurethane plastic wastes. Five different types of postconsumer plastic wastes, namely, landfill liners, medicine bottles, packaging materials, and two different industrial plastic wastes, were used. The noncatalytic cracking caused by pyrolysis at 600 °C yielded products that helped to identify the major polymer present in the plastic wastes. The pyrolysis experiments were also conducted in the presence of different catalysts based on our previous work. The results showed that the addition of a catalyst greatly influenced the product compositions, which might have resulted from the interactions of different impurities or additives present in plastic wastes. Therefore, catalysts can have a significant effect on the selectivity of a specific compound. Furthermore, the temperature used for the catalytic pyrolysis also showed an effect on the product compositions. This study demonstrated the high sensitivity of the technique to detect the presence of polymer material present in the plastic waste and the impurities present. This information can be used to aid in designing the pyrolysis process on a large scale.

In addition, a batch-scale pyrolysis validation of landfill liner plastic waste was demonstrated, and the liquid product obtained, i.e., plastic crude oil, was fractionated into different fractions (gasoline range, aviation range fuel, and gas oil plus range fraction). A detailed characterization of various fractions was performed. Fuel property analysis of the aviation range fuel fraction obtained from the PCO-LL and its comparison with a commercial jet fuel showed that this fraction exhibited characteristics of jet fuel. The data suggest that the produced plastic crude oil has the potential to be co-processed in refineries with petroleum crude oil to produce fuels for various applications.

Supplementary Materials: The following supporting information can be downloaded at: <https://www.mdpi.com/article/10.3390/en15238821/s1>, Figure S1: ¹H-NMR-spectra of distillate fractions i.e., gasoline range (<150 °C); aviation range fuel (150–275 °C); gas oil plus range (>275 °C) obtained after pyrolysis of landfill liner (LL) plastic waste. Comparison with commercial jet fuel is also presented.

Author Contributions: Conceptualization, B.K.S.; methodology, B.K. and S.R.C.; validation, K.K., R.P., S.R.C. and B.K.S.; formal analysis, B.K., S.R.C. and B.R.M.; investigation, K.K. and R.P.; writing—original draft preparation, K.K., R.P. and S.R.C.; writing—review and editing, K.K., R.P., B.R.M., S.A.-S. and B.K.S.; supervision, B.K.S.; project administration, B.K.S. All authors have read and agreed to the published version of the manuscript.

Funding: This study was funded by the Environmental Research and Education Foundation (807 EREF 2013-00296) and partly by the Hazardous Waste Research Fund of ISTC, PRI.

Data Availability Statement: Not applicable.

Acknowledgments: The authors thank the Environmental Research and Education Foundation and Hazardous Waste Research Fund of ISTC, PRI for their financial support.

Conflicts of Interest: The authors declare no conflict of interest.

References

1. Guglielmi, G. In the next 30 years, we'll make four times more plastic waste than we ever have. *Science* **2017**. [CrossRef]
2. Geyer, R.; Jambeck, J.R.; Law, K.L. Production, use, and fate of all plastics ever made. *Sci. Adv.* **2017**, *3*, 1700782. [CrossRef] [PubMed]
3. United States Environmental Protection Agency Office of Solid Waste (5306P) Municipal Solid Waste in The United States, EPA530-R-13-001 (2013). Available online: <https://archive.epa.gov/epawaste/nonhaz/municipal/web/html/msw99.html> (accessed on 17 February 2022).

4. Hoornweg, D.; Bhada-Tata, P.; Kennedy, C. Environment: Waste production must peak this century. *Nature* **2013**, *502*, 615–616. [CrossRef] [PubMed]
5. Kaza, S.; Yao, L.; Bhada-Tata, P.; Van Woerden, F. *What a Waste 2.0: A Global Snapshot of Solid Waste Management to 2050*; International Bank for Reconstruction and Development/The World Bank: Washington, DC, USA, 2018; p. 29. ISBN 978-1-4648-1329-0. Available online: <https://openknowledge.worldbank.org/handle/10986/30317> (accessed on 17 February 2022).
6. Bagri, R.; Williams, P.T. Catalytic pyrolysis of polyethylene. *J. Anal. Appl. Pyrolysis* **2012**, *63*, 29–41. [CrossRef]
7. Williams, P.T.; Williams, E.A. Fluidised bed pyrolysis of low-density polyethylene to produce petrochemical feedstock. *J. Anal. Appl. Pyrolysis* **1999**, *51*, 107–126. [CrossRef]
8. Liu, Y.; Qian, J.; Wang, J. Pyrolysis of polystyrene waste in a fluidized-bed reactor to obtain styrene monomer and gasoline fraction. *Fuel Process. Technol.* **2000**, *63*, 45–55. [CrossRef]
9. Williams, E.A.; Williams, P.T. Analysis of products derived from the fast pyrolysis of plastic waste. *J. Anal. Appl. Pyrolysis* **1997**, *40*, 347–363. [CrossRef]
10. Williams, J.H.; Williams, P.T. Analysis of products from the pyrolysis of plastics recovered from the commercial scale recycling of waste electrical and electronic equipment. *J. Anal. Appl. Pyrolysis* **2007**, *79*, 375–386. [CrossRef]
11. Miandad, R.; Barakat, M.A.; Aburizaiza, A.S.; Rehan, M.; Nizami, A.S. Catalytic pyrolysis of plastic waste: A review. *Process Saf. Environ. Prot.* **2016**, *102*, 822–838. [CrossRef]
12. Adrados, A.; de Marco, I.; Caballero, B.M.; López, A.; Laresgoiti, M.F.; Torres, A. Pyrolysis of plastic packaging waste: A comparison of plastic residuals from material recovery facilities with simulated plastic waste. *Waste Manag.* **2012**, *32*, 826–832. [CrossRef]
13. López, A.; de Marco, I.; Caballero, B.M.; Adrados, A.; Laresgoiti, M.F. Deactivation and regeneration of ZSM-5 zeolite in catalytic pyrolysis of plastic wastes. *Waste Manag.* **2011**, *31*, 1852–1858. [CrossRef] [PubMed]
14. Chandrasekaran, S.R.; Kunwar, B.; Moser, B.R.; Rajagopalan, N.; Sharma, B.K. Catalytic thermal cracking of postconsumer waste plastics to fuels. 1. Kinetics and Optimization. *Energy Fuels* **2015**, *29*, 6068–6077. [CrossRef]
15. Zhang, X.; Lei, H.; Yadavalli, G.; Zhu, L.; Wei, Y.; Liu, Y. Gasoline-range hydrocarbons produced from microwave-induced pyrolysis of low-density polyethylene over ZSM-5. *Fuel* **2015**, *144*, 33–42. [CrossRef]
16. Auxilio, A.R.; Choo, W.; Kohli, I.; Srivatsa, S.C.; Bhattacharya, S. An experimental study on thermo-catalytic pyrolysis of plastic waste using a continuous pyrolyzer. *Waste Manag.* **2017**, *67*, 143–154. [CrossRef] [PubMed]
17. Lee, H.W.; Park, Y.K. Catalytic pyrolysis of polyethylene and polypropylene over desilicated beta and Al-MSU-F. *Catalysts* **2018**, *8*, 501. [CrossRef]
18. Jia, C.; Xie, S.; Zhang, W.; Intan, N.N.; Sampath, J.; Pfaendtner, J.; Lin, H. Deconstruction of high-density polyethylene into liquid hydrocarbon fuels and lubricants by hydrogenolysis over Ru catalyst. *Chem Catal.* **2021**, *1*, 437–455. [CrossRef]
19. Tomasek, S.; Varga, Z.; Hancsok, J. Production of jet fuel from cracked fractions of waste polypropylene and polyethylene. *Fuel Process. Technol.* **2020**, *197*, 106197. [CrossRef]
20. Peng, Y.; Wang, Y.; Ke, L.; Dai, L.; Wu, Q.; Cobb, K.; Zeng, Y.; Zou, R.; Liu, Y.; Ruan, R. A review on catalytic pyrolysis of plastic wastes to high-value products. *Energy Convers. Manag.* **2022**, *254*, 115243. [CrossRef]
21. Dai, L.; Zhou, N.; Lv, Y.; Cheng, Y.; Wang, Y.; Liu, Y.; Cobb, K.; Chen, P.; Lei, H.; Ruan, R. Pyrolysis technology for plastic waste recycling: A state-of-the-art review. *Prog. Energy Combust. Sci.* **2022**, *93*, 101021. [CrossRef]
22. Yusuf, A.A.; Ampah, J.D.; Soudagar, E.M.; Veza, I.; Kingsley, U.; Afrane, S.; Jin, C.; Liu, H.; Elfakhany, A.; Buyondo, K.A. Effect of hybrid nanoparticle additives in n-butanol/waste plastic oil/diesel blends on combustion, particulate and gaseous emissions from diesel engine evaluated with entropy-weighted PROMETHEE II and TOPSIS: Environmental and health risks of plastic waste. *Energy Convers. Manag.* **2022**, *264*, 115758. [CrossRef]
23. Rocha-Santos, T.; Duarte, A.C. A critical overview of the analytical approaches to the occurrence, the fate and the behavior of microplastics in the environment. *Trends Anal. Chem.* **2015**, *65*, 47–53. [CrossRef]
24. Frère, L.; Paul-Pont, I.; Moreau, J.; Soudant, P.; Lambert, C.; Huvet, A.; Rinnert, E. A semi-automated Raman micro-spectroscopy method for morphological and chemical characterizations of microplastic litter. *Mar. Pollut. Bull.* **2016**, *113*, 461–468. [CrossRef]
25. Camacho, W.; Karlsson, S. NIR, DSC, and FTIR as quantitative methods for compositional analysis of blends of polymers obtained from recycled mixed plastic wastes. *Polym. Eng. Sci.* **2001**, *41*, 1626–1635. [CrossRef]
26. Hummel, D.O.; Scholl, F.K. *Atlas of Polymer and Plastics Analysis V.2: Plastics, Fibers, Rubbers, Resins, Starting and Auxiliary Materials, Degradation Products*; Carl Hanser Verlag Chemie GmbH (Wiley-VCH GmbH): Weinheim, Germany, 1988. [CrossRef]
27. Hallensleben, M.L.; Rambke, J. Photoresponsive polymers, 2,4-vinylazobenzene, a new polymerizable azo-monomer, Die Makromolekulare Chemie. *Rapid Commun.* **1989**, *10*, 559–562. [CrossRef]
28. Kusch, P.; Knupp, G. Headspace-SPME-GC-MS identification of volatile organic compounds released from expanded polystyrene. *J. Polym. Environ.* **2004**, *12*, 83–87. [CrossRef]
29. Wampler, T.P. *Applied Pyrolysis Handbook*; CRC Press: Boca Raton, FL, USA, 2006. [CrossRef]
30. Moldoveanu, S. *Analytical Pyrolysis of Synthetic Organic Polymers*; Elsevier: Amsterdam, The Netherlands, 2005; Volume 25. [CrossRef]
31. Yang, M.; Shibasaki, Y. Mechanisms of thermal degradation of polystyrene, polymethacrylonitrile, and their copolymers on flash pyrolysis. *J. Polym. Sci. Part A Polym. Chem.* **1998**, *36*, 2315–2330. [CrossRef]

32. Sharma, B.K.; Moser, B.R.; Vermillion, K.E.; Doll, K.M.; Rajagopalan, N. Production, characterization and fuel properties of alternative diesel fuel from pyrolysis of waste plastic grocery bags. *Fuel Process. Technol.* **2014**, *122*, 79–90. [\[CrossRef\]](#)
33. Kunwar, B.; Moser, B.R.; Chandrasekaran, S.R.; Rajagopalan, N.; Sharma, B.K. Catalytic and thermal depolymerization of low value post-consumer high density polyethylene plastic. *Energy* **2016**, *111*, 884–892. [\[CrossRef\]](#)
34. Suarez, P.A.Z.; Moser, B.R.; Sharma, B.K.; Erhan, S.Z. Comparing the lubricity of biofuels obtained from pyrolysis and alcoholysis of soybean oil and their blends with petroleum diesel. *Fuel* **2009**, *88*, 1143–1147. [\[CrossRef\]](#)
35. Moser, B.R.; Williams, A.; Haas, M.J.; McCormick, R.L. Exhaust emissions and fuel properties of partially hydrogenated soybean oil methyl esters blended with ultra-low sulfur diesel fuel. *Fuel Process. Technol.* **2009**, *90*, 1122–1128. [\[CrossRef\]](#)
36. Moser, B.R. Impact of fatty ester composition on low temperature properties of biodiesel-petroleum diesel blends. *Fuel* **2014**, *115*, 500–506. [\[CrossRef\]](#)
37. Doll, K.M.; Moser, B.R.; Erhan, S.Z. Surface tension studies of alkyl esters and epoxidized alkyl esters relevant to oleochemically based fuel additives. *Energy Fuels* **2007**, *21*, 3044–3048. [\[CrossRef\]](#)
38. Manos, G.; Garforth, A.; Dwyer, J. Thermolysis of low-density polyethylene catalyzed by zeolites. *J. Anal. Appl. Pyrolysis* **1994**, *29*, 45–55.
39. Costa, P.A.; Pinto, F.J.; Ramos, A.M.; Gulyurtlu, I.K.; Cabrita, I.A.; Bernardo, M.S. Kinetic evaluation of the pyrolysis of polyethylene waste. *Energy Fuels* **2007**, *21*, 2489–2498. [\[CrossRef\]](#)
40. Rizzarelli, P.; Rapisarda, M.; Perna, S.; Mirabella, E.F.; La Carta, S.; Puglisi, C.; Valenti, G. Determination of polyethylene in biodegradable polymer blends and in compostable carrier bags by Py-GC/MS and TGA. *J. Anal. Appl. Pyrolysis* **2016**, *117*, 72–81. [\[CrossRef\]](#)
41. De Stefanis, A.; Cafarelli, P.; Gallese, F.; Borsella, E.; Nana, A.; Perez, G. Catalytic pyrolysis of polyethylene: A comparison between pillared and restructured clays. *J. Anal. Appl. Pyrolysis* **2013**, *104*, 479–484. [\[CrossRef\]](#)
42. Leclerc, P.; Doucet, J.; Chaoukia, J. Development of a microwave thermogravimetric analyzer and its application on polystyrene microwave pyrolysis kinetics. *J. Anal. Appl. Pyrolysis* **2018**, *130*, 209–215. [\[CrossRef\]](#)
43. Ballice, L.; Reimert, R. Classification of volatile products from the temperature-programmed pyrolysis of polypropylene (PP) atactic-polypropylene (APP) and thermogravimetrically derived kinetics of pyrolysis. *Chem. Eng. Process. Process Intensif.* **2002**, *41*, 289–296. [\[CrossRef\]](#)
44. Audisio, G.; Silvani, A. Catalytic thermal degradation of polymers degradation of polypropylene. *J. Anal. Appl. Pyrolysis* **1984**, *7*, 83–90. [\[CrossRef\]](#)
45. Ojha, D.K.; Vinu, R. Resource recovery via catalytic fast pyrolysis of polystyrene using zeolite. *J. Anal. Appl. Pyrolysis* **2015**, *113*, 349–359. [\[CrossRef\]](#)
46. Zhou, X.; Broadbelt, L.J.; Vinu, R. Mechanistic understanding of thermochemical conversion of Polymers and lignocellulosic biomass. *Adv. Chem. Eng.* **2016**, *49*, 95–198. [\[CrossRef\]](#)
47. Fabbri, D.; Trombini, C.; Vassura, I. Analysis of polystyrene in polluted sediments by pyrolysis-gas chromatography-mass spectroscopy. *J. Chromatogr. Sci.* **1998**, *36*, 600–604. [\[CrossRef\]](#)
48. Lin, R.; White, R.L. Acid-catalyzed cracking of polystyrene. *J. Appl. Polym. Sci.* **1997**, *63*, 1287–1298. [\[CrossRef\]](#)
49. Lattimer, R.P.; Polce, M.J.; Wesdemiotis, C. MALDI-MS analysis of pyrolysis products from a segmented polyurethane. *J. Anal. Appl. Pyrolysis* **1998**, *48*, 1–15. [\[CrossRef\]](#)
50. Hileman, F.D.; Voorhees, K.J.; Wojcik, L.H. Pyrolysis of a flexible urethane foam. *J. Polym. Sci. Polym. Chem. Ed.* **1975**, *13*, 571–584. [\[CrossRef\]](#)
51. Font, R.; Fullana, A.; Caballero, J.A.; Candela, J.; Garcia, A. Pyrolysis study of polyurethane. *J. Anal. Appl. Pyrolysis* **2001**, *58*, 63–77. [\[CrossRef\]](#)
52. Jiao, L.; Xiao, H.; Wang, Q.; Sun, J. Thermal degradation characteristics of rigid polyurethane foam and volatile products analysis with TG-FTIR-MS. *Polym. Degrad. Stab.* **2013**, *98*, 2687–2696. [\[CrossRef\]](#)
53. Dyer, E.; Wright, G.C. Thermal degradation of alkyl N-phenylcarbamates. *J. Am. Chem. Soc.* **1959**, *81*, 2138–2143. [\[CrossRef\]](#)
54. Williams, P.T.; Williams, E.A. Interaction of plastics in mixed-plastics pyrolysis. *Energy Fuels* **1999**, *13*, 188–196. [\[CrossRef\]](#)
55. Pinto, F.; Costa, P.; Gulyurtlu, I.; Cabrita, I. Pyrolysis of plastic wastes. 1. Effect of plastic waste composition of product yield. *J. Anal. Appl. Pyrolysis* **1999**, *51*, 39–55. [\[CrossRef\]](#)
56. Kizza, R.; Bonadda, N.; Seay, J. Qualitative and energy recovery potential analysis: Plastic-derived fuel oil versus conventional diesel oil. *Clean Technol. Environ. Policy* **2022**, *24*, 789–800. [\[CrossRef\]](#)
57. Marcilla, A.; Gomez, A.; Garcia, A.N.; Olaya, M.M. Kinetic study of the catalytic decomposition of different commercial polyethylenes over an MCM-41 catalyst. *J. Anal. Appl. Pyrolysis* **2002**, *64*, 85–101. [\[CrossRef\]](#)
58. de la Puente, G.; Sedran, U. Recycling polystyrene into fuels by means of FCC: Performance of various acidic catalyst. *Appl. Catal. B Environ.* **1998**, *19*, 305–311. [\[CrossRef\]](#)
59. Mertinkat, J.; Predel, L.; Kaminsky, W. Cracking catalysts used as fluidized bed material in Hamburg pyrolysis process. *J. Anal. Appl. Pyrolysis* **1999**, *49*, 87–95. [\[CrossRef\]](#)
60. Faravelli, T.; Bozzano, G.; Colombo, M.; Ranzi, E.; Dente, M. Kinetic modeling of thermal degradation of polyethylene and polystyrene mixtures. *J. Anal. Appl. Pyrolysis* **2003**, *70*, 761–777. [\[CrossRef\]](#)